

# Sub-Riemannian Geometry in Image Processing and Modelling of Human Visual System



**Alexey Mashtakov**

Program Systems Institute of RAS

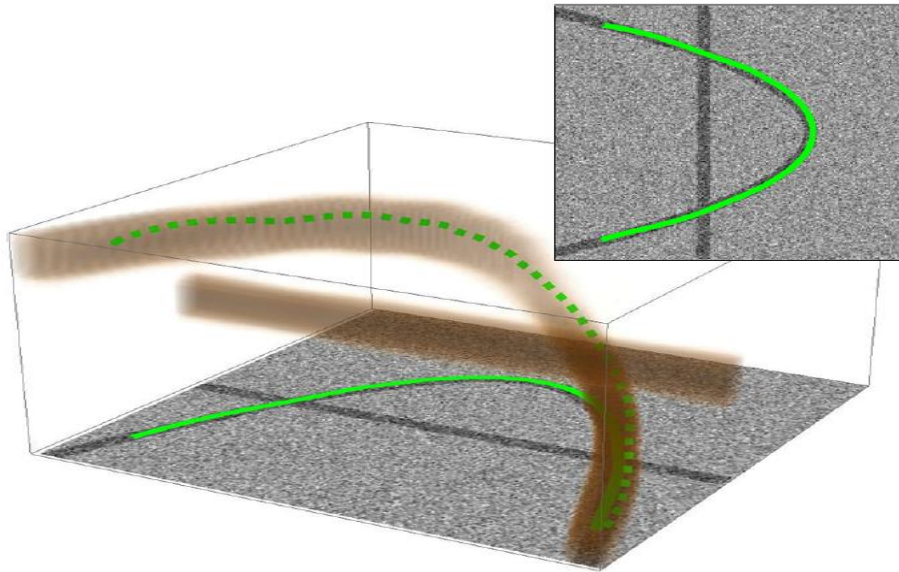


Based on joint works with

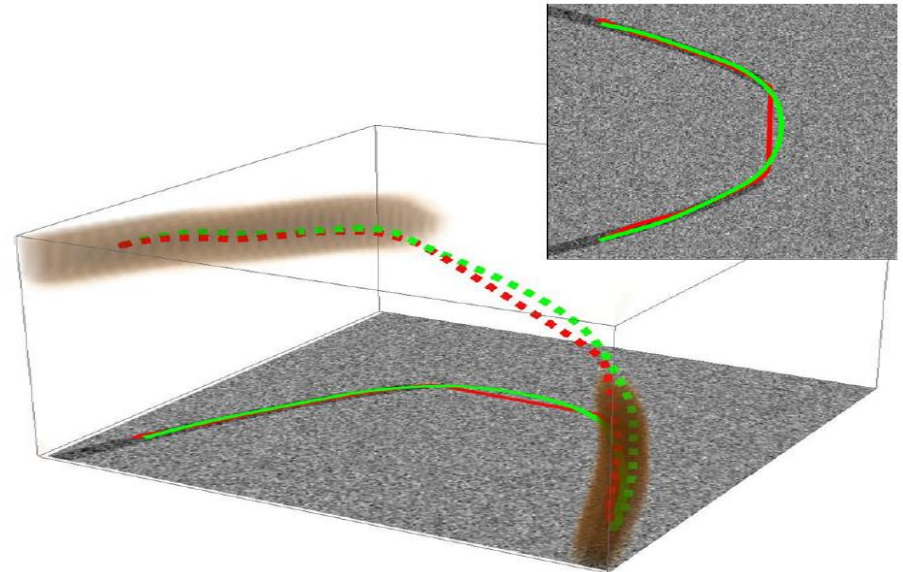
R. Duits, Yu. Sachkov, G. Citti, A. Sarti, A. Popov  
E. Bekkers, G. Sanguinetti, A. Ardentov, B. Franceschiello  
I. Beschastnyi, A. Ghosh and T.C.J. Dela Haije

International conference on Geometric Analysis in honor of the  
90th anniversary of academician Yu. G. Reshetnyak  
Novosibirsk, Russia, 25.09.2019

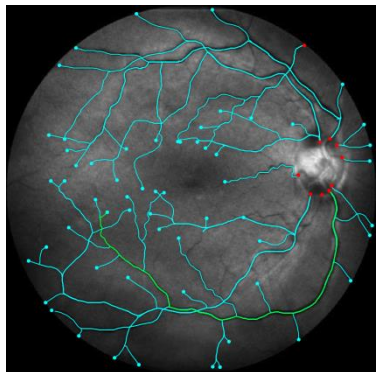
# Sub-Riemannian geodesics on Lie Groups



Crossing structures are disentangled



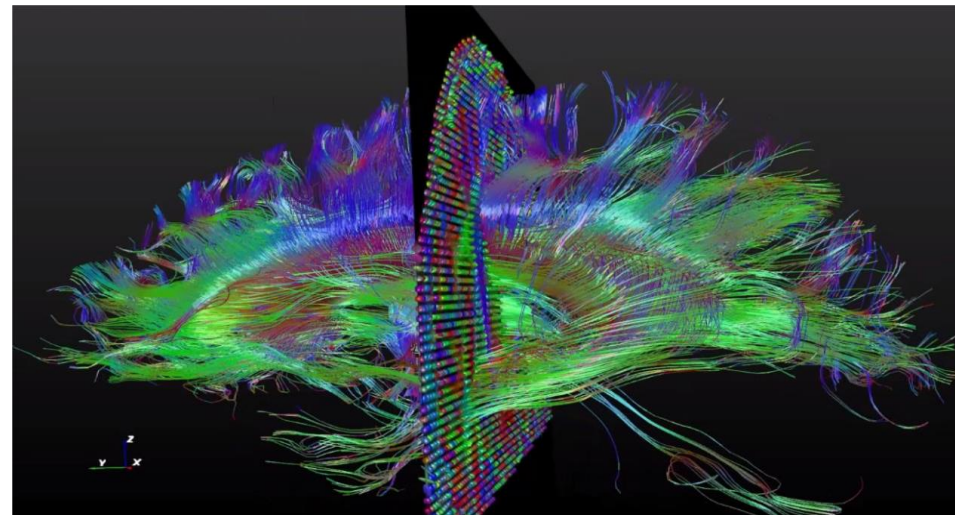
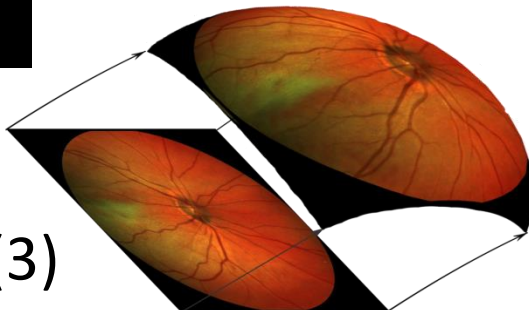
Reconstruction of corrupted contours based on model of human vision



Applications in medical image analysis

$SE(2)$

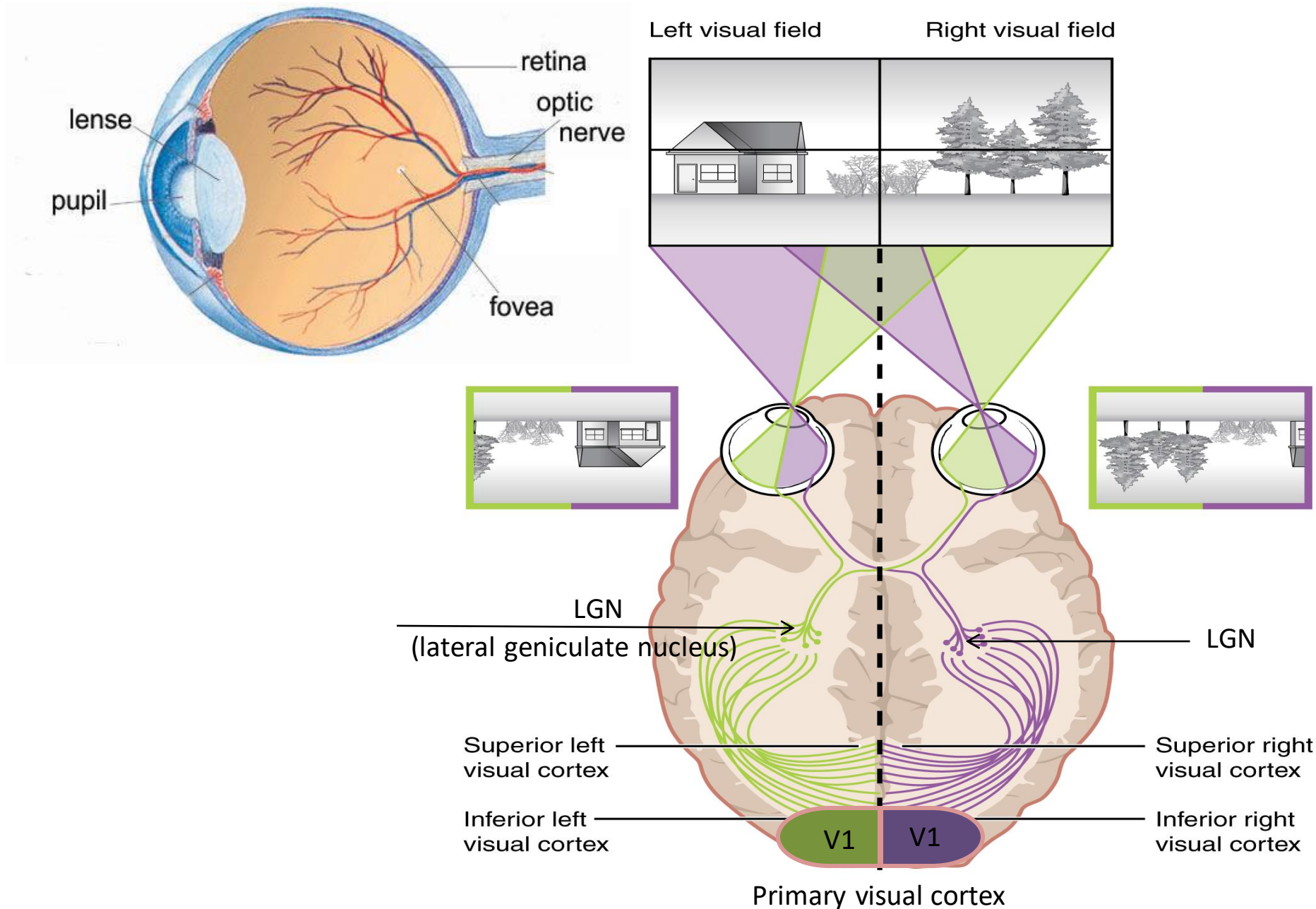
$SO(3)$



$SE(3)$

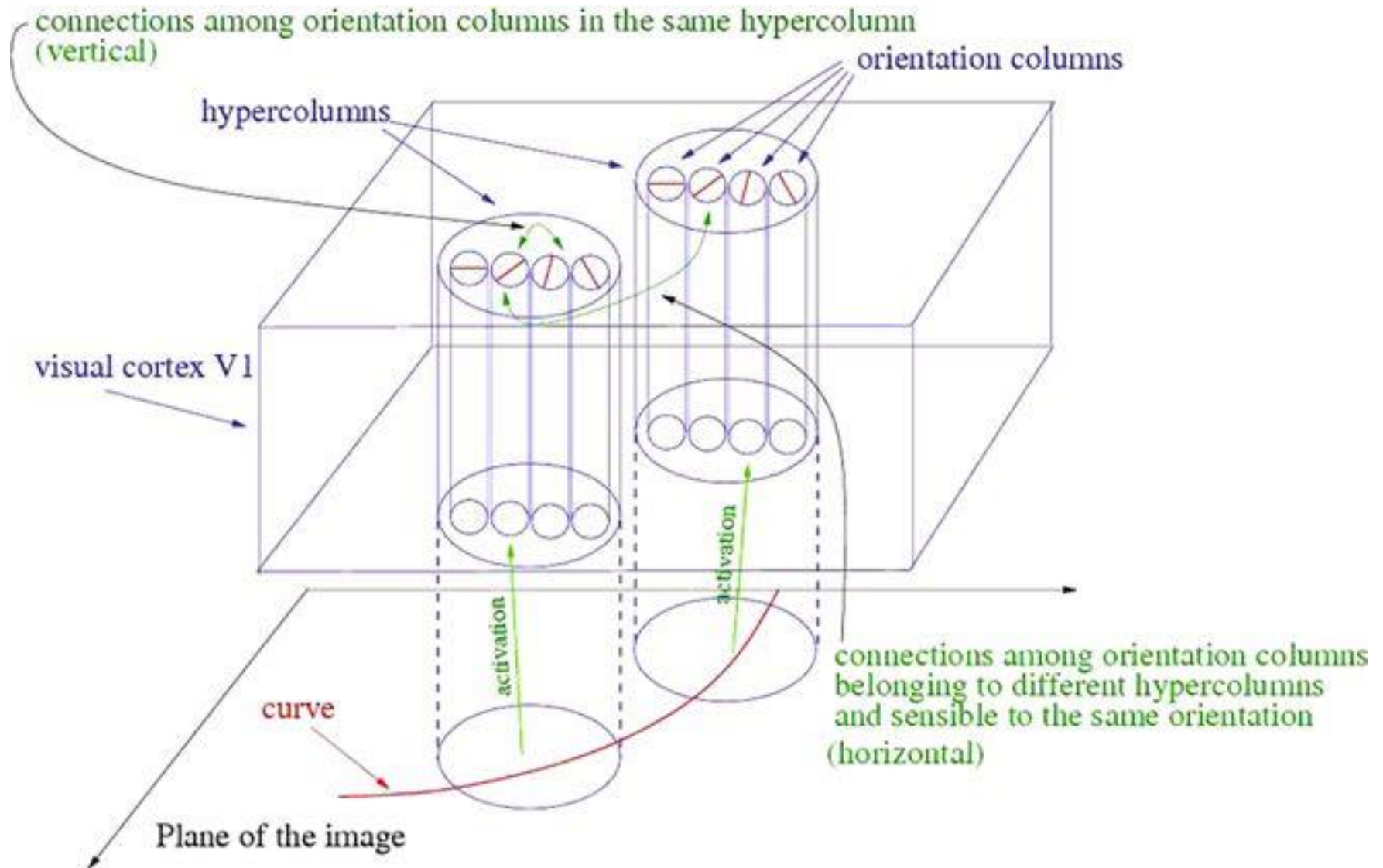
# Sub-Riemannian Geometry in Modelling of Vision

# Perception of Visual Information by Human Brain





# A Model of the Primary Visual Cortex V1

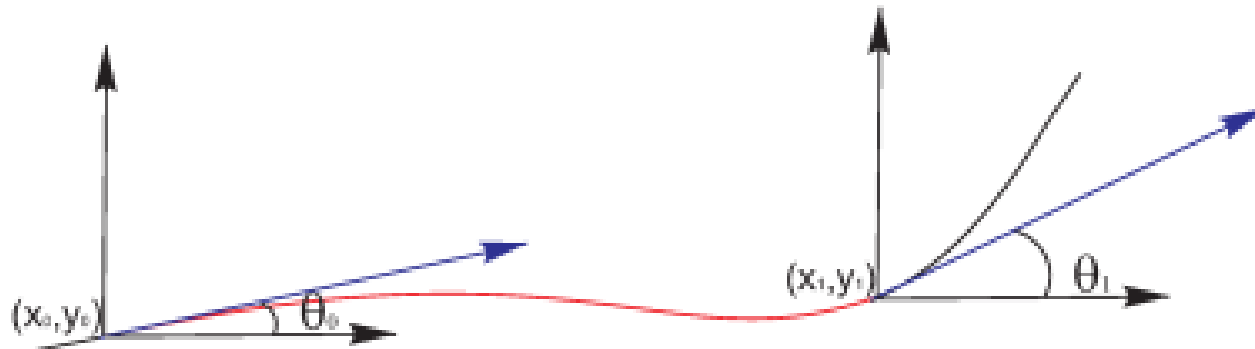


Replicated from R. Duits, U. Boscain, F. Rossi, Y. Sachkov,  
Association Fields via Cuspless Sub-Riemannian Geodesics in  $SE(2)$ , JMIV, 2013.

# Cortical Based Model of Perceptual Completion

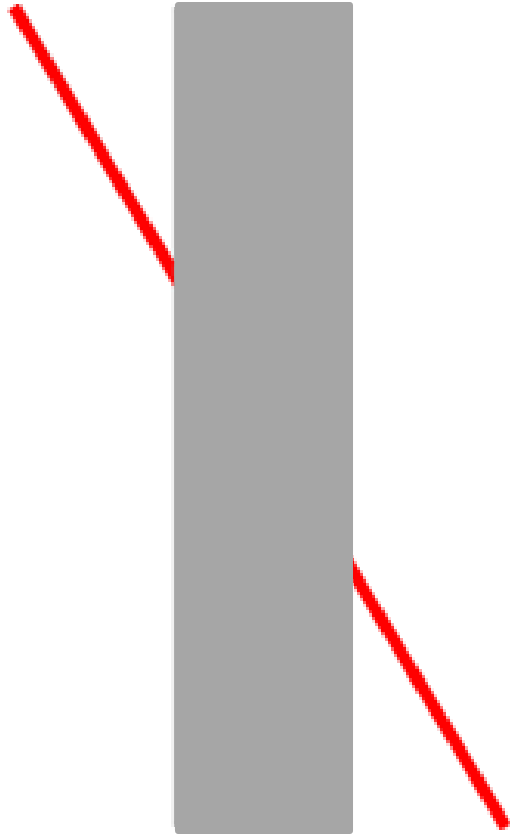
- D.H. Hubel and T.N. Wiesel, Receptive fields of single neurones in the cat's striate cortex, 1959. Nobel prize in 1981.
- Sub-Riemannian structures in neurogeometry of the vision:
  - J. Petitot, The neurogeometry of pinwheels as a sub-Riemannian contact structure, 2003. (Heisenberg group.)
  - G. Citti and A. Sarti, A Cortical Based Model of Perceptual Completion in the Roto-Translation Space, 2006. ( $SE(2)$  group.)
- Variational principle: recovered arc has minimal length in the space  $(x, y, \theta)$ :

$$\int \sqrt{\xi^2 (\dot{x}^2 + \dot{y}^2) + \dot{\theta}^2} dt \rightarrow \min, \text{ under constraint } \dot{\theta} = \arg(\dot{x} + i \dot{y})$$

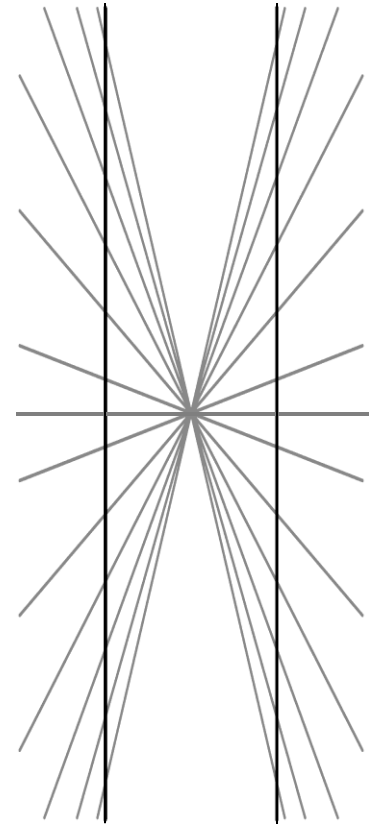


# Geometrical Optical Illusions

---



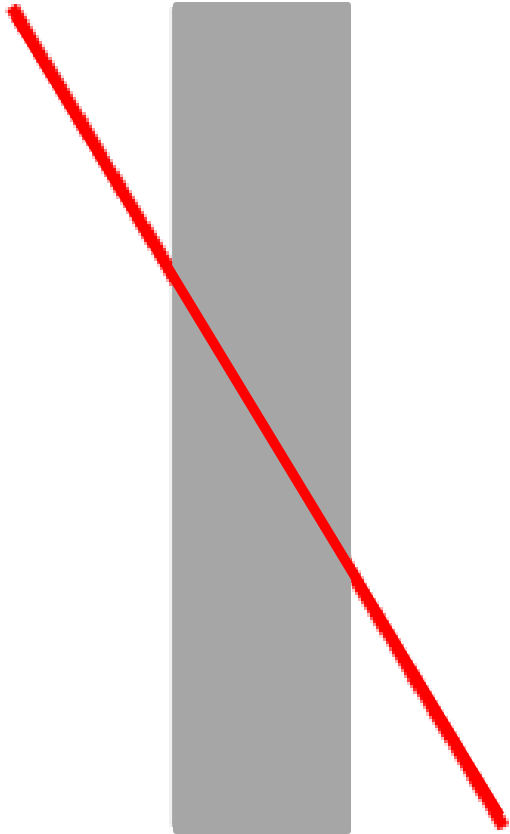
Poggendorff illusion



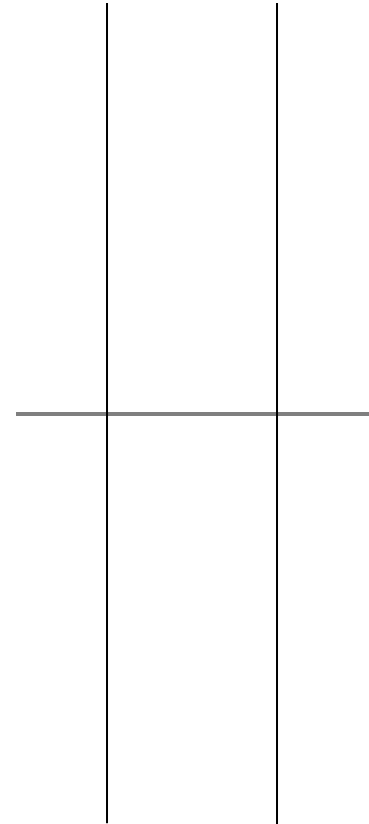
Hering illusion

# Geometrical Optical Illusions

---



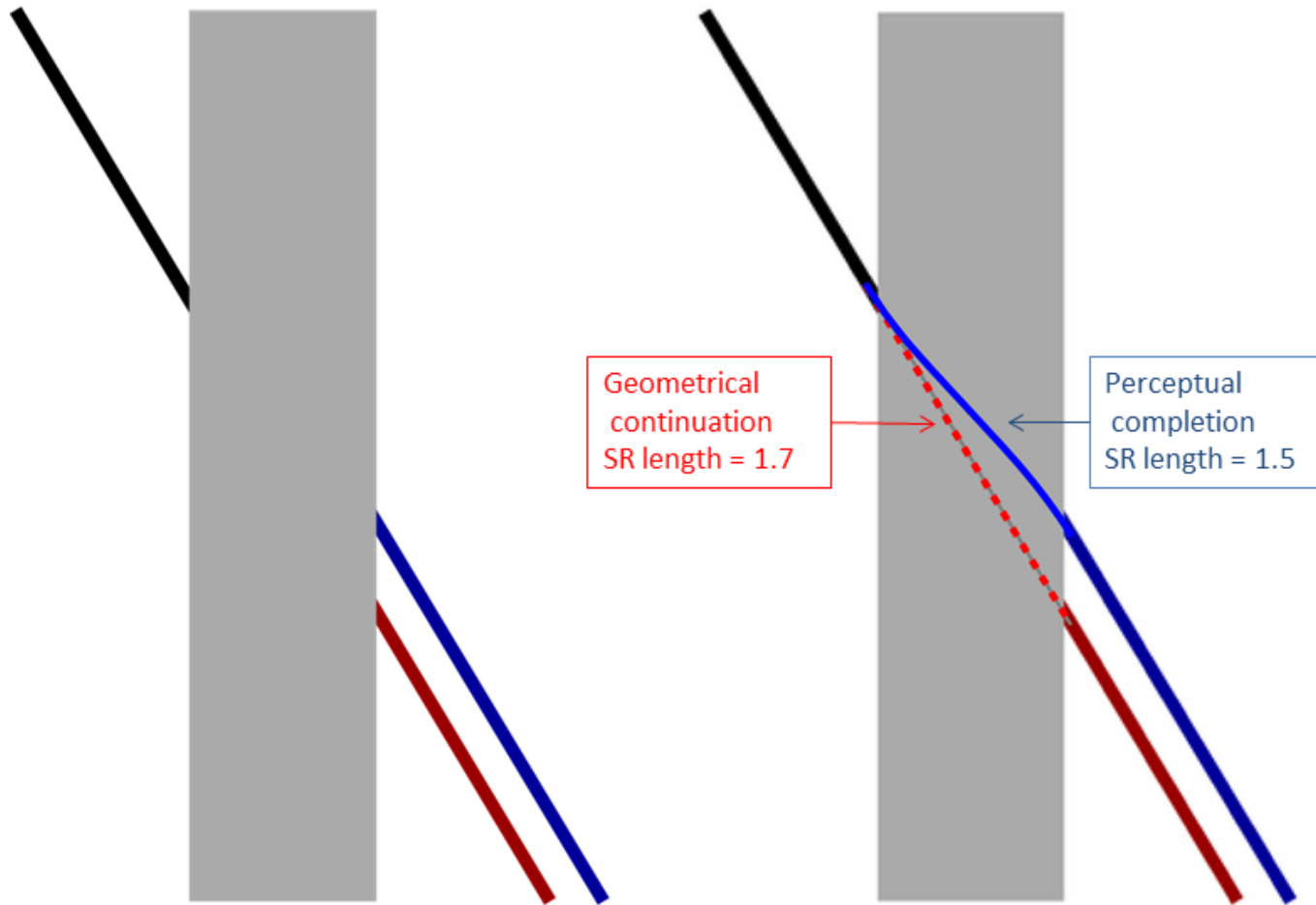
Poggendorff illusion



Hering illusion



# Modelling of Illusory Contour



Idea: The illusory contour appears as a geodesic in a metric induced by visual stimulus.

# Brief Tour in Sub-Riemannian Geometry

# Left-invariant sub-Riemannian structures

- $G$  – Lie group,  $e$  – unit element  
 $\Delta \subset TG$  – left invariant subbundle of tangent bundle,  
 $\mathcal{G}$  – left-invariant inner product in  $\Delta$ .
- $\gamma : [0, T] \rightarrow G$  – horizontal (i.e. admissible) curve if

$$\dot{\gamma}(t) \in \Delta_{\gamma(t)} \text{ for a.e. } t \in [0, T].$$

SR length minimizers are horizontal curves  $\gamma$  that have minimum length

$$l(\gamma) = \int_0^T \sqrt{\mathcal{G}(\dot{\gamma}(t), \dot{\gamma}(t))} dt \rightarrow \min.$$

- Left-invariant contact sub-Riemannian structure on  $d(d+1)/2$  Lie group:  
 $(G, \Delta, \mathcal{G})$ ,  $\Delta = \text{span}(\mathcal{A}_1, \dots, \mathcal{A}_d)$ ,  $\mathcal{G}(\mathcal{A}_i, \mathcal{A}_j) = \delta_{ij}$ .  
Here  $\mathcal{A}_1, \dots, \mathcal{A}_d$  are left-invariant vector fields on  $G$ , s.t.

$$\Delta + [\Delta, \Delta] = TG.$$

# Optimal Control Problem: ODE-based Approach

- Optimal Control Problem

$$\dot{\gamma}(t) = u_1(t) \mathcal{A}_1|_{\gamma(t)} + \dots + u_d(t) \mathcal{A}_d|_{\gamma(t)}$$

$$\gamma(0) = e, \quad \gamma(T) = g_1$$

$$l(\gamma) = \int_0^T \sqrt{u_1(t)^2 + \dots + u_d(t)^2} dt \rightarrow \min$$
$$(u_1(t), \dots, u_d(t)) \in \mathbb{R}^d,$$

- Pontryagin Maximum Principle: the Hamiltonian system

$$\dot{\lambda} = \vec{H}(\lambda), \quad \lambda \in T^*G$$

- Exponential mapping:

$$\text{Exp} : (\lambda_0, t) \mapsto \gamma(t)$$

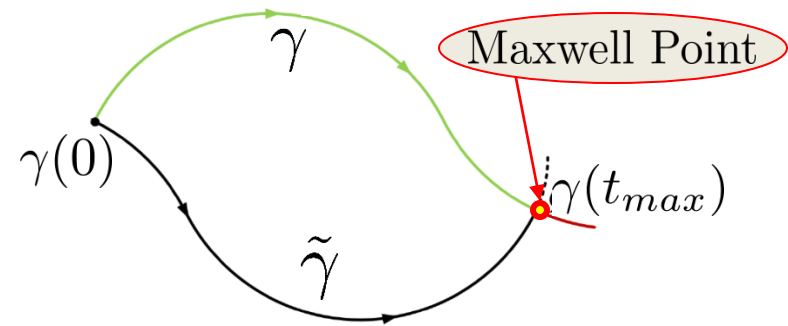
# Optimality of Extremal Trajectories

- Short arcs of extremal trajectories  $\gamma$  are optimal
- Cut time along  $\gamma$ :

$$t_{cut} = \sup\{\tau > 0 \mid \gamma(t) \text{ is optimal for } t \in [0, \tau]\}.$$

- Maxwell time  $t_{max}$ :

$$\exists \tilde{\gamma} \neq \gamma : \begin{cases} \gamma(0) = \tilde{\gamma}(0), \\ \gamma(t_{max}) = \tilde{\gamma}(t_{max}) \end{cases}$$



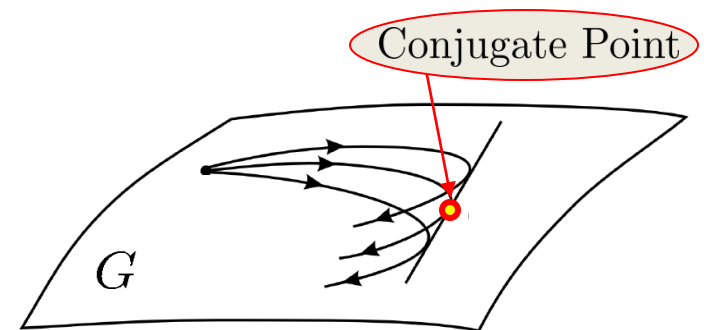
- Conjugate time  $t_{conj}$ :

Conjugate point – critical value of Exp:

$$\frac{\partial \text{Exp}}{\partial (\lambda, t)}(\lambda_0, t_{conj}) = 0.$$

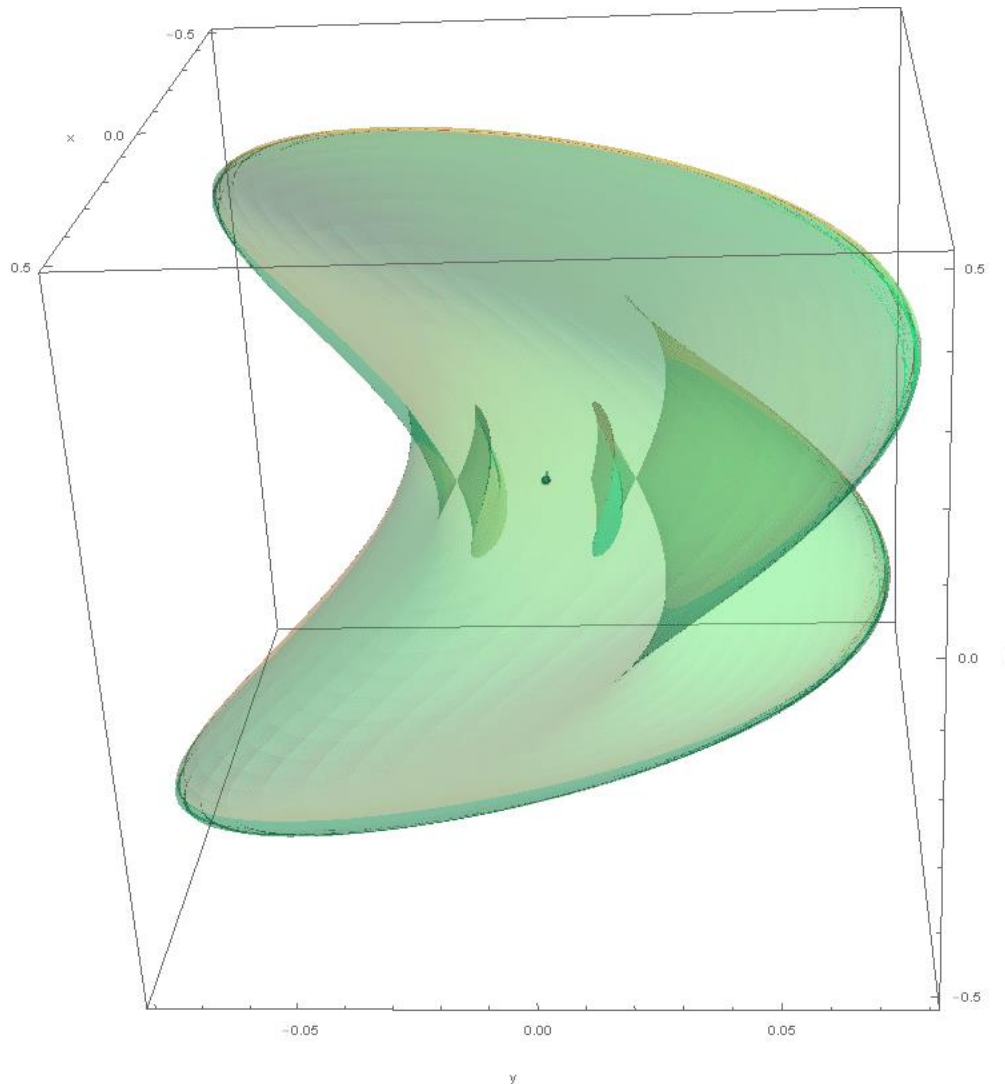
- Upper bound on cut time:

$$t_{cut} \leq \min(t_{max}, t_{conj}).$$



# Sub-Riemannian Wave Front

$$W(T) = \{\text{Exp}(\lambda_0, T) | \lambda_0 \in T_e^*G, H(\lambda_0) = \tfrac{1}{2}\}.$$



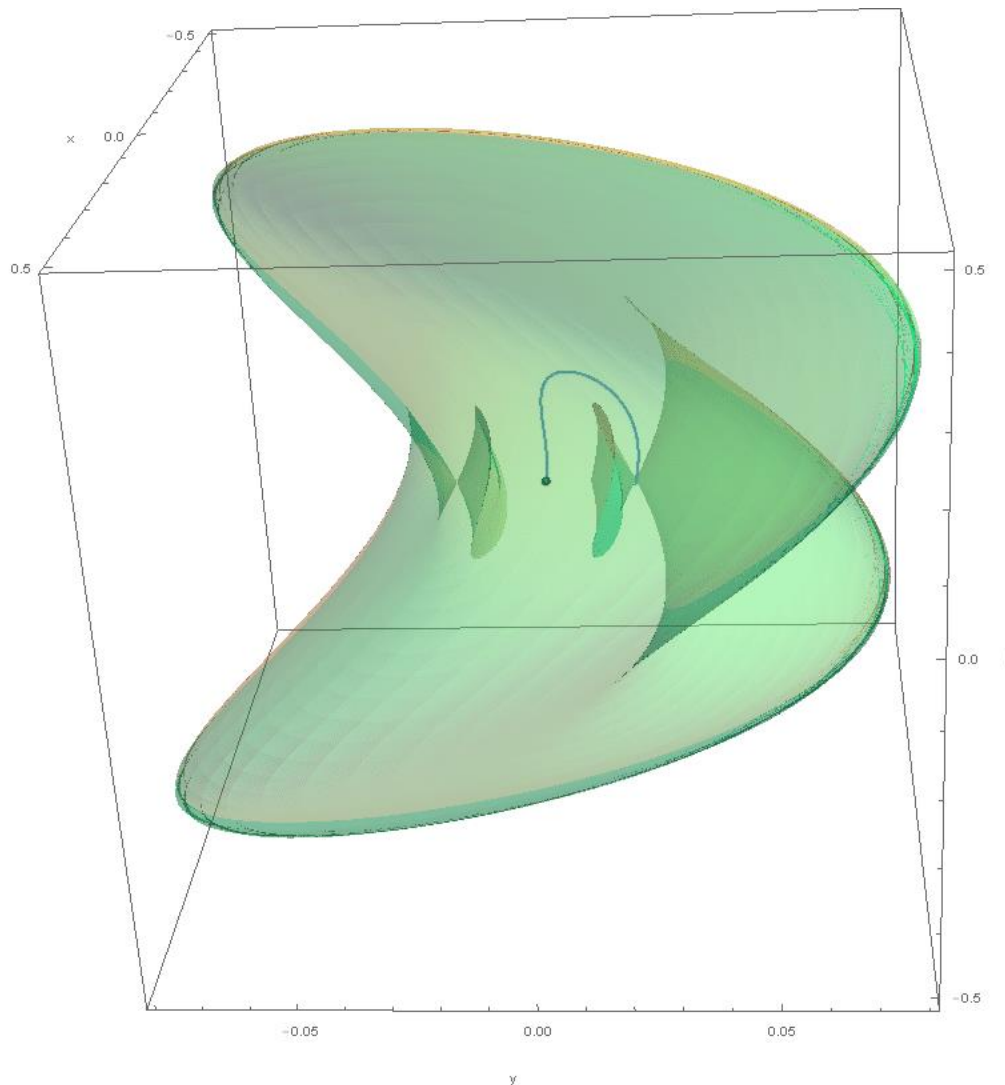
$$\lambda_0 = (\nu_0, c_0)$$

Varying  $t$   
 $\Rightarrow$   
one geodesic



# Sub-Riemannian Wave Front

$$W(T) = \{\text{Exp}(\lambda_0, T) | \lambda_0 \in T_e^*G, H(\lambda_0) = \frac{1}{2}\}.$$

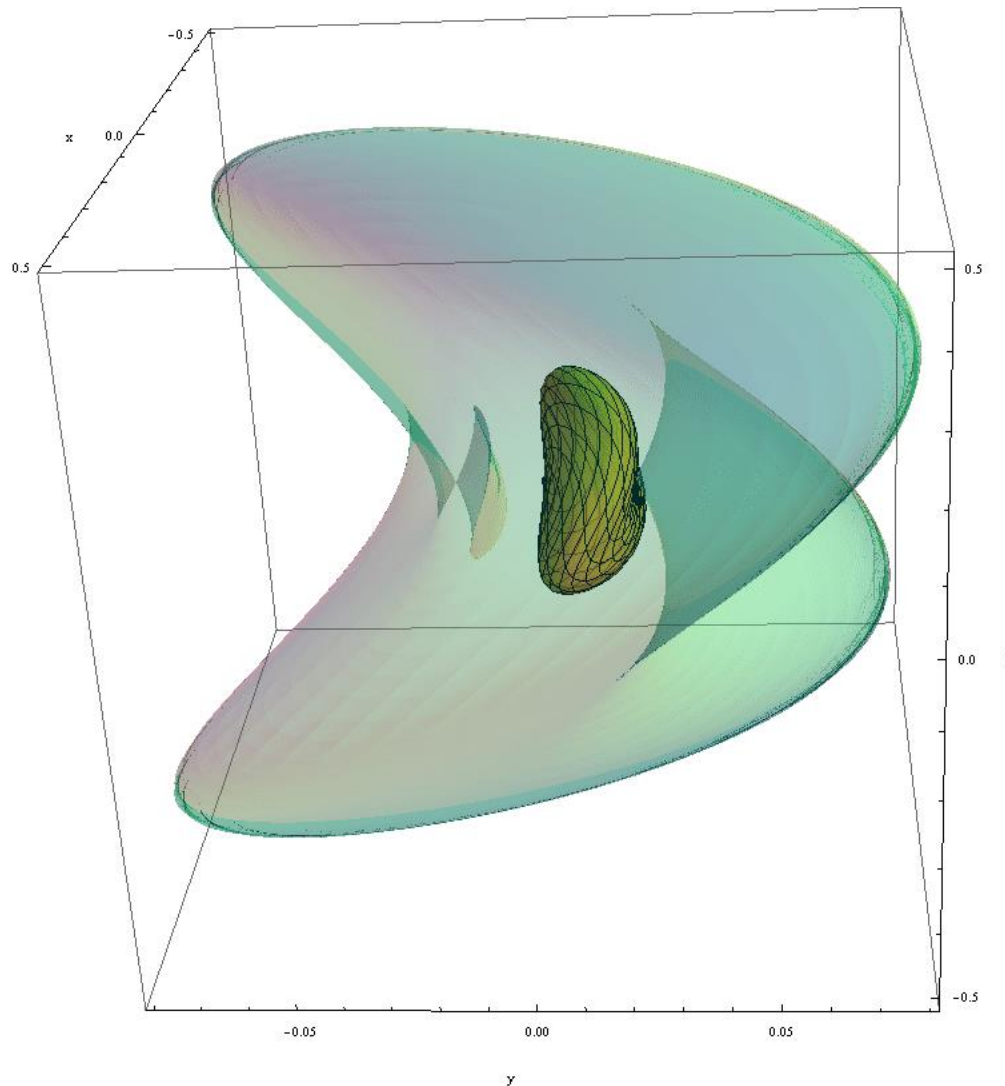


$$\lambda_0 = (\nu_0, c_0)$$

$t \in [0, T]$   
Varying  $\nu_0$   
 $\Rightarrow$  family of  
geodesics

# Sub-Riemannian Wave Front

$$W(T) = \{\text{Exp}(\lambda_0, T) | \lambda_0 \in T_e^*G, H(\lambda_0) = \tfrac{1}{2}\}.$$



$$\lambda_0 = (\nu_0, c_0)$$

$$t \in [0, T]$$

$$2\nu_0 \in S^1$$

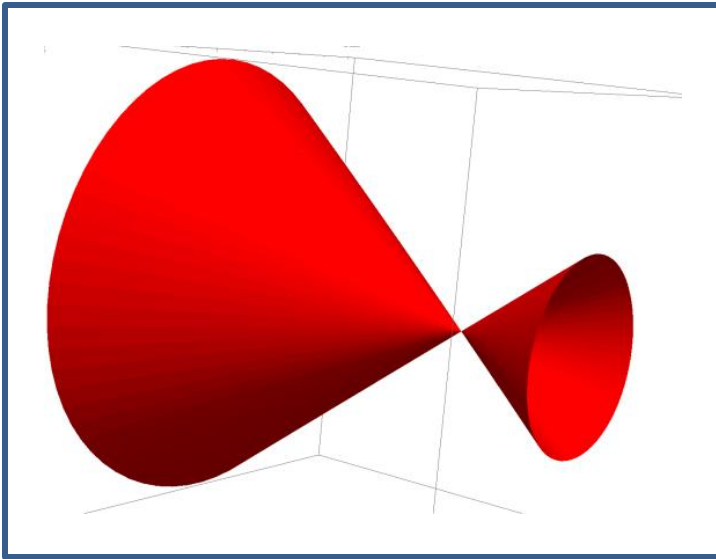
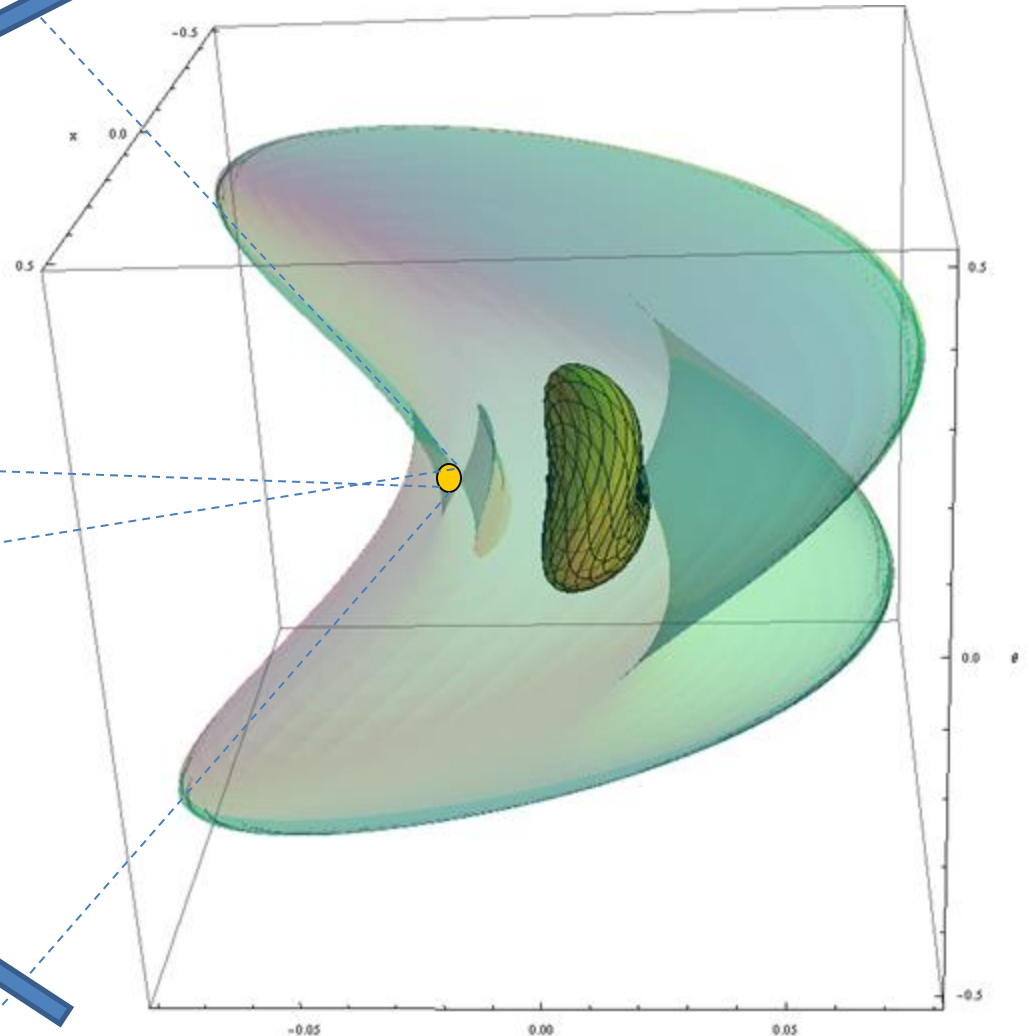
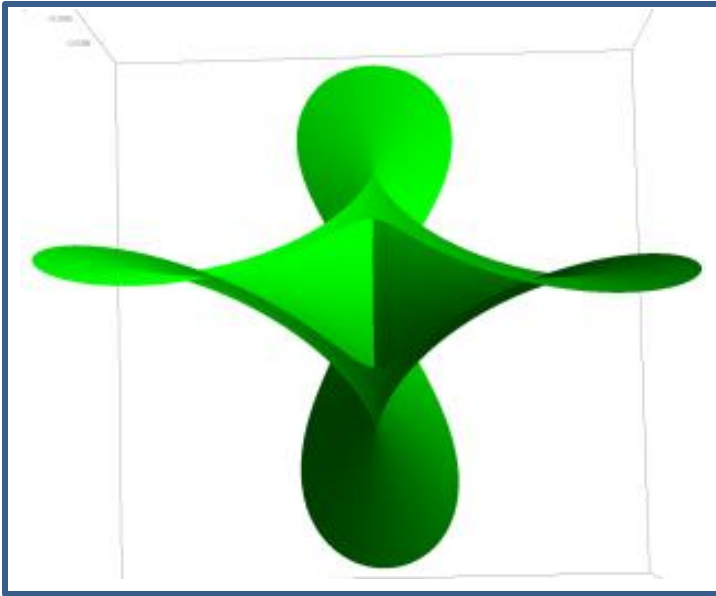
Varying  $c_0$

$\Rightarrow$

whole family  
of geodesics

# Self intersection of Sub-Riemannian Wave Front

General case: astroidal shape of conjugate locus



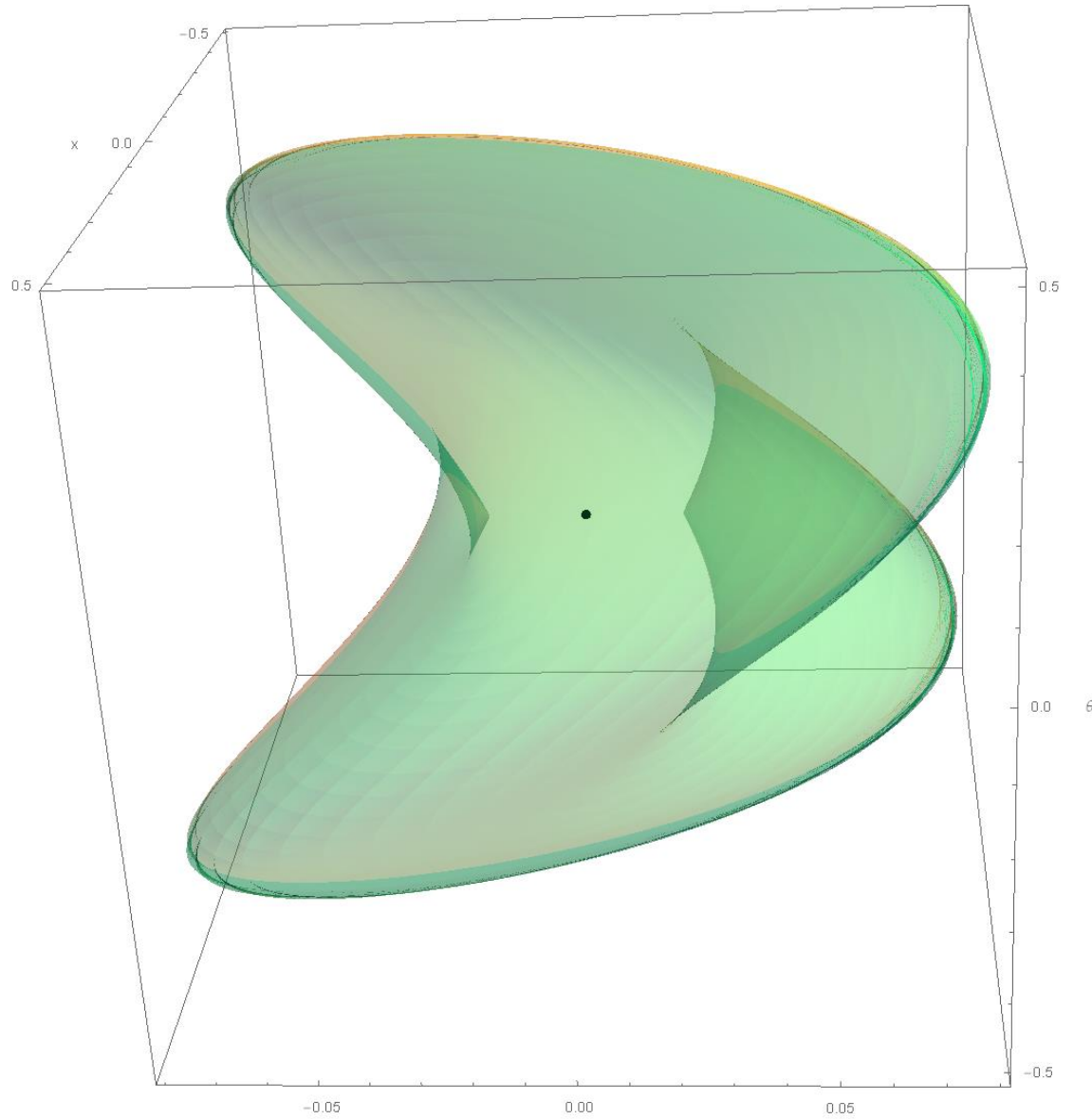
Special case with rotational symmetry

A.Agrachev, Exponential mappings for contact sub-Riemannian structures. JDCS, 1996.

H. Chakir, J.P. Gauthier and I. Kupka, Small Subriemannian Balls on  $R^3$ . JDCS, 1996.

# Sub-Riemannian Sphere

$$S(T) = \{\text{Exp}(\lambda_0, T) | \lambda_0 \in T_e^*G, H(\lambda_0) = \frac{1}{2}, t_{cut}(\lambda_0) \geq T\}.$$



# Sub-Riemannian Length Minimizers

## Problem Statement.

$$\dot{\gamma} = \sum_{i=1}^d u_i \mathcal{A}_i, \quad \gamma(0) = e, \gamma(T) = g, \quad l(\gamma) = \int_0^T \mathcal{C}(\gamma(t)) \sqrt{\sum_{i=1}^d u_i^2(t)} dt \rightarrow \min$$

**Theorem.** Let  $\mathcal{W}(g)$  be a viscosity solution of eikonal system

$$\begin{cases} \sum_{i=1}^d (\mathcal{A}_i|_g(\mathcal{W}))^2 = \mathcal{C}^2(g), & \text{for } g \neq e, \\ \mathcal{W}(e) = 0. \end{cases}$$

Then

- $\mathcal{W}(g) = d(e, g)$  is the SR distance map;
- $\mathcal{S}_t = \{g \in G \mid \mathcal{W}(g) = t\}$  are SR-spheres  $S(t)$  of radius  $t$ ;
- SR-minimizer  $\gamma(t)$  connecting  $e$  to  $g$  is given by  $\gamma(t) = \gamma_b(\mathcal{W}(g) - t)$ , where  $\gamma_b(t)$  is found by integration for  $t \in [0, \mathcal{W}(g)]$

$$\dot{\gamma}_b(t) = -u_1(t) \mathcal{A}_1|_{\gamma_b(t)} - \dots - u_d(t) \mathcal{A}_d|_{\gamma_b(t)}, \quad \gamma_b(0) = g,$$

$$\text{where } u_i(t) = \frac{\mathcal{A}_i|_{\gamma_b(t)}(\mathcal{W})}{\mathcal{C}^2(\gamma_b(t))}, \quad i = 1, \dots, d.$$

# Detection of salient curves in images



# Analysis of Images of the Retina

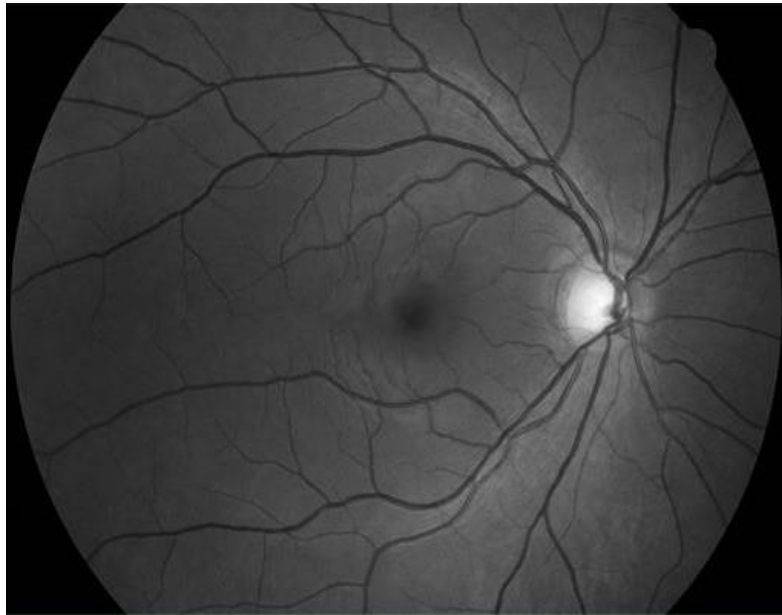
Diabetic retinopathy --- one of the main causes of blindness.

Epidemic forms: 10% people in China suffer from DR.

Patients are found early --> treatment is well possible.

Early warning --- leakage and malformation of blood vessels.

The retina --- excellent view on the microvasculature of the brain.



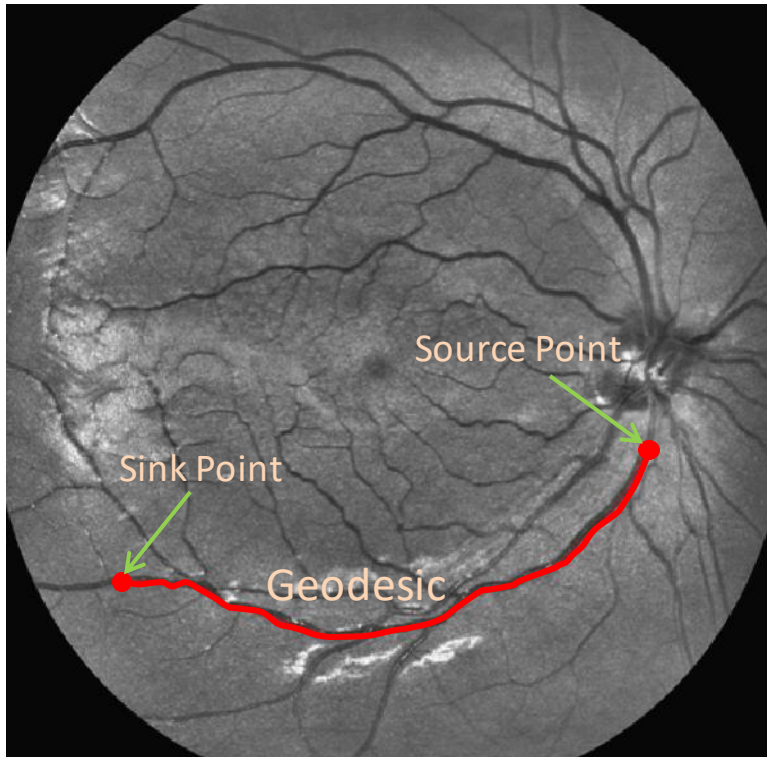
Healthy retina



Diabetes Retinopathy with  
tortuous vessels

# Geodesic Methods in Computer Vision

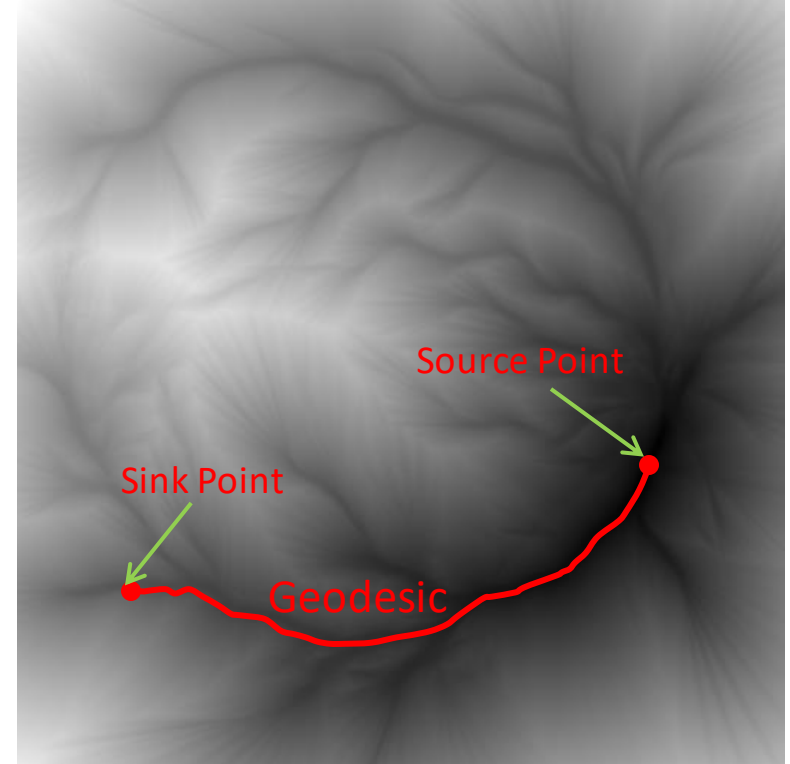
Image



Tracking of salient lines via data-driven minimal paths (or geodesics).

Data-driven **Geodesic** – curve that minimizes length functional weighted by external cost (function with high values at image locations with high curve saliency).

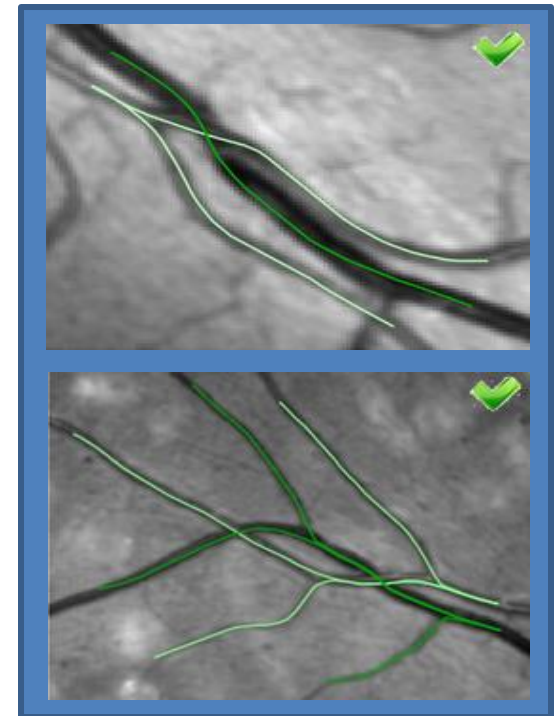
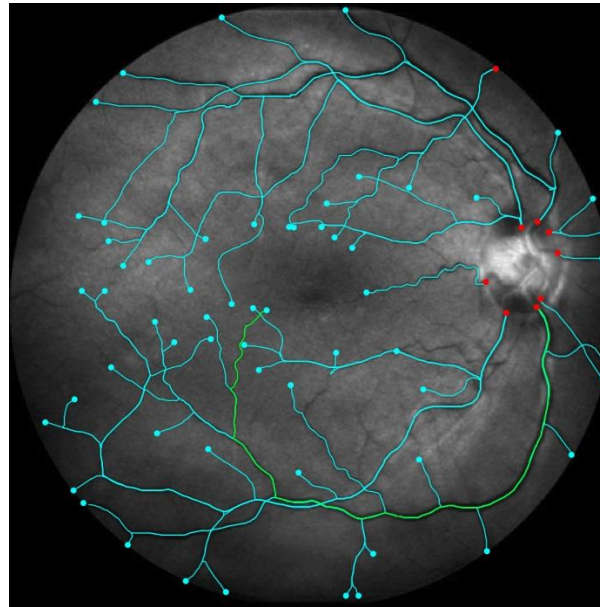
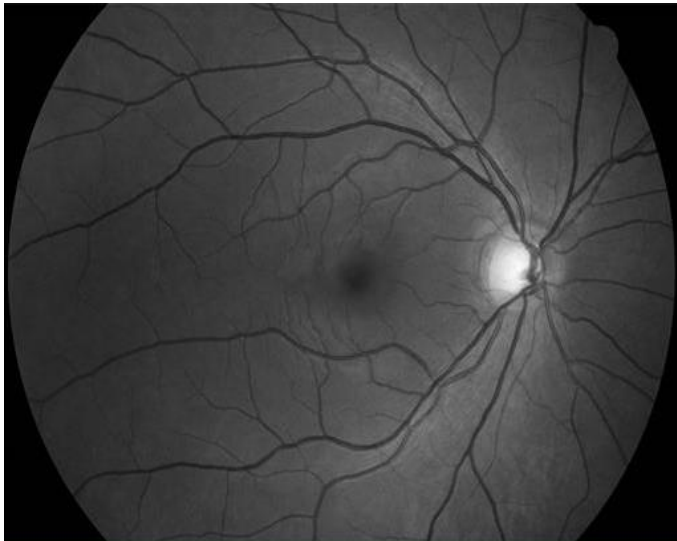
Distance from source point



Fast Marching method to compute geodesics:

- 1) Computation of distance map from source point,
- 2) Geodesic via steepest decent on distance map.

# Tracking of Lines in Flat Images via Sub-Riemannian Geodesics in $SE(2)$

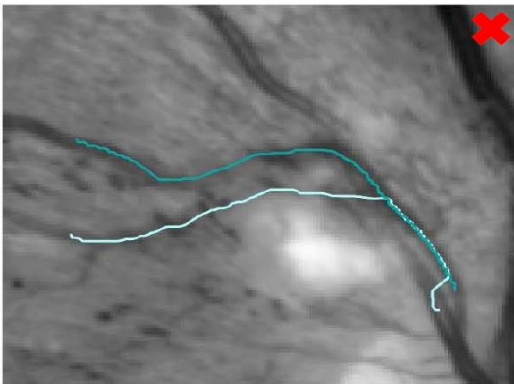
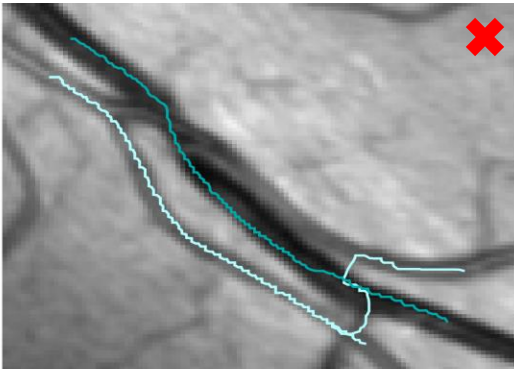
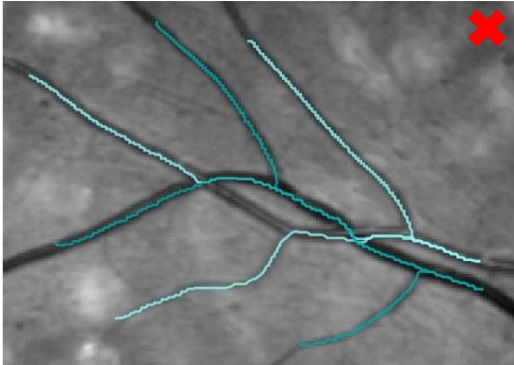


- [1] E.J. Bekkers, R. Duits, A. Mashtakov and G.R. Sanguinetti, *Data-driven Sub-Riemannian Geodesics in  $SE(2)$* , Proc. SSVM, 2015.
- [2] E.J. Bekkers, R. Duits, A. Mashtakov and G.R. Sanguinetti, *A PDE Approach to Data-driven Sub-Riemannian Geodesics in  $SE(2)$* , SIIMS, 2015.
- [3] G. Sanguinetti, R. Duits, E. Bekkers, M. Janssen, A. Mashtakov, J-M. Mirebeau, *Sub-Riemannian Fast Marching in  $SE(2)$* , Proc. CIARP, 2015.

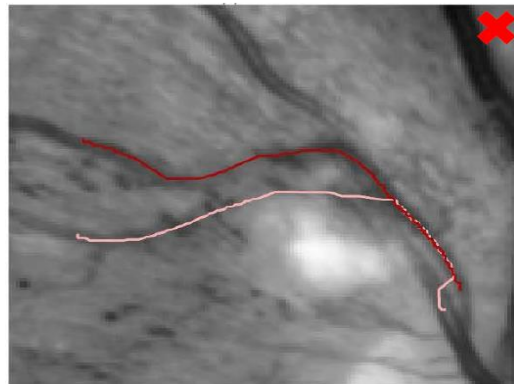
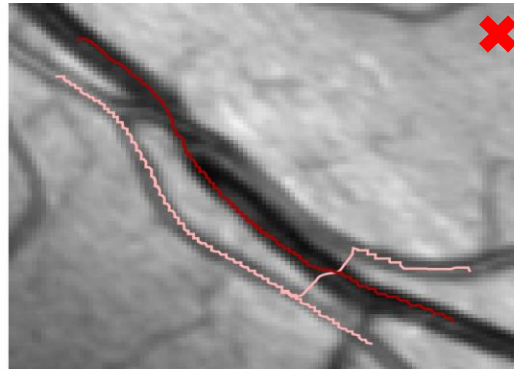
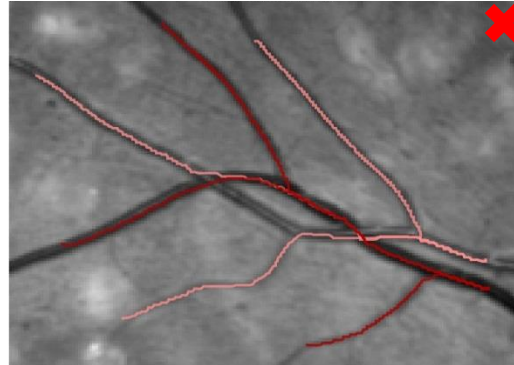


# Comparison with Classical Methods

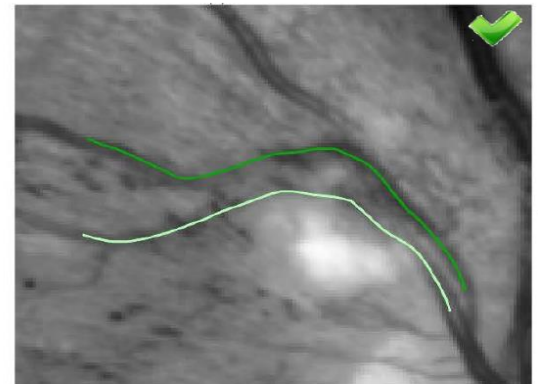
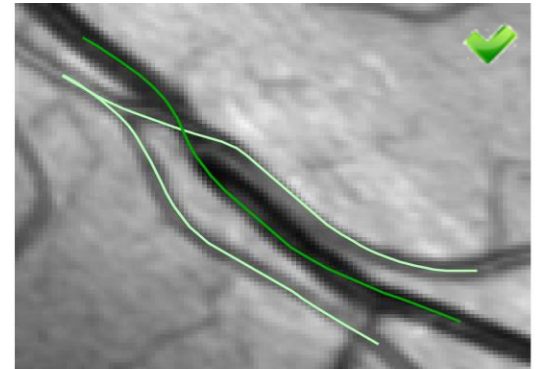
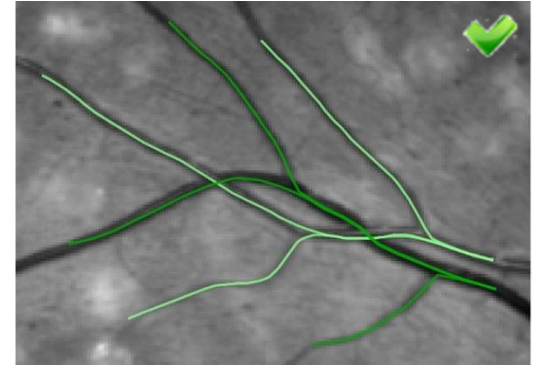
$\mathbb{R}^2$  - Riemannian



$SE(2)$  - Riemannian

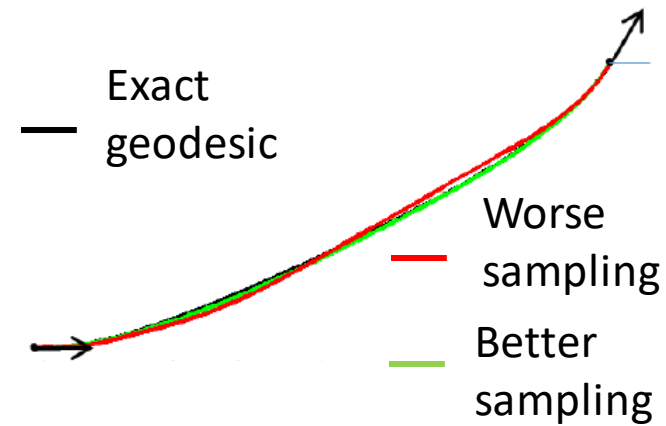


$SE(2)$  - Sub-Riemannian

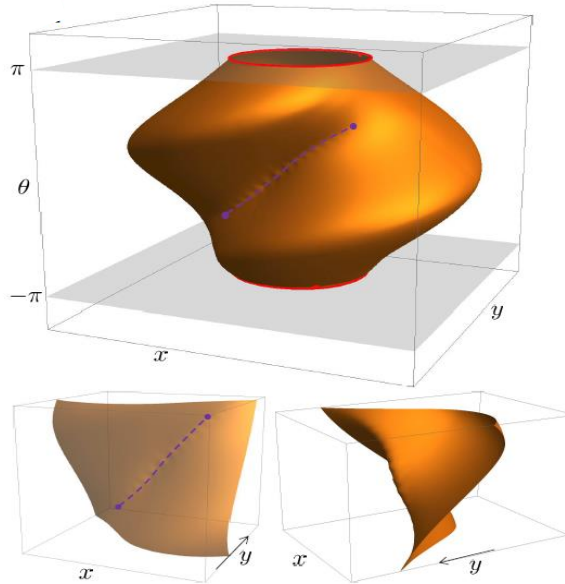


# Numerical Verification for $C=1$

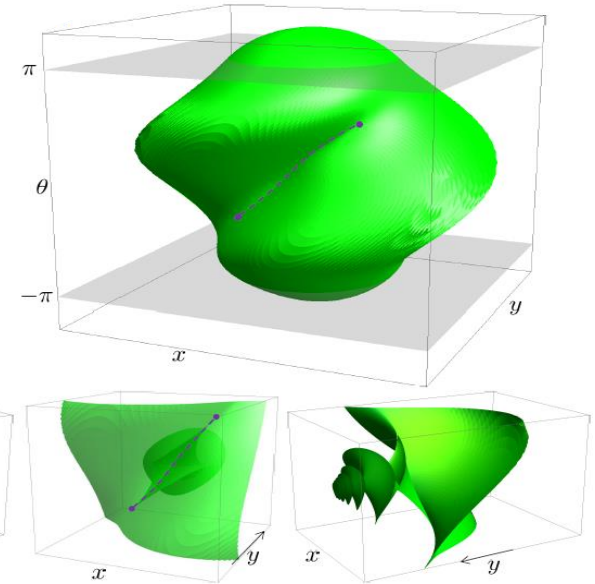
## Converging to Exact Geodesics



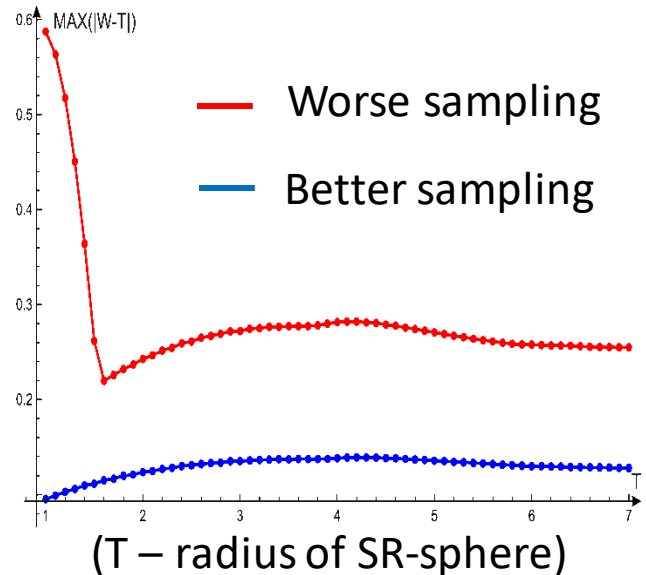
## SR-sphere Numerically



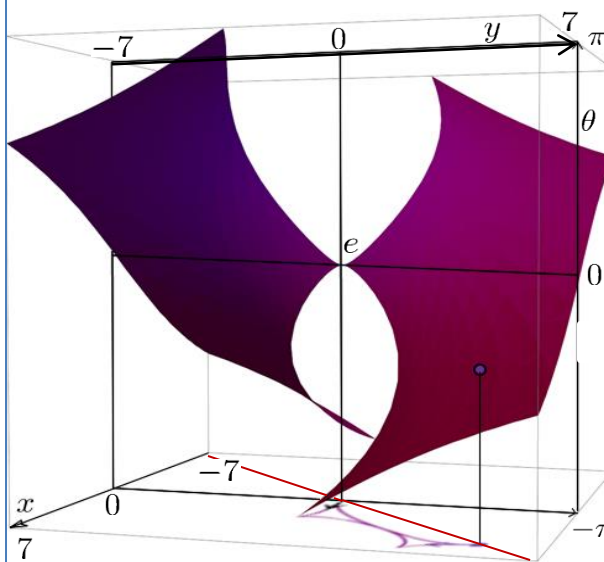
## Exact Wavefront



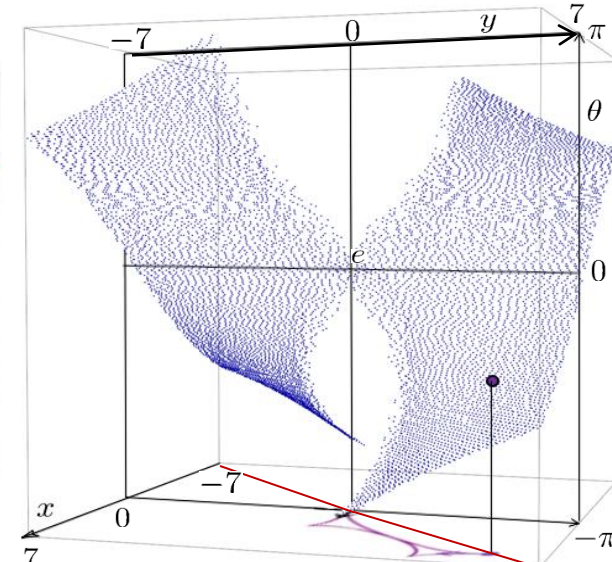
## Max Absolute Error



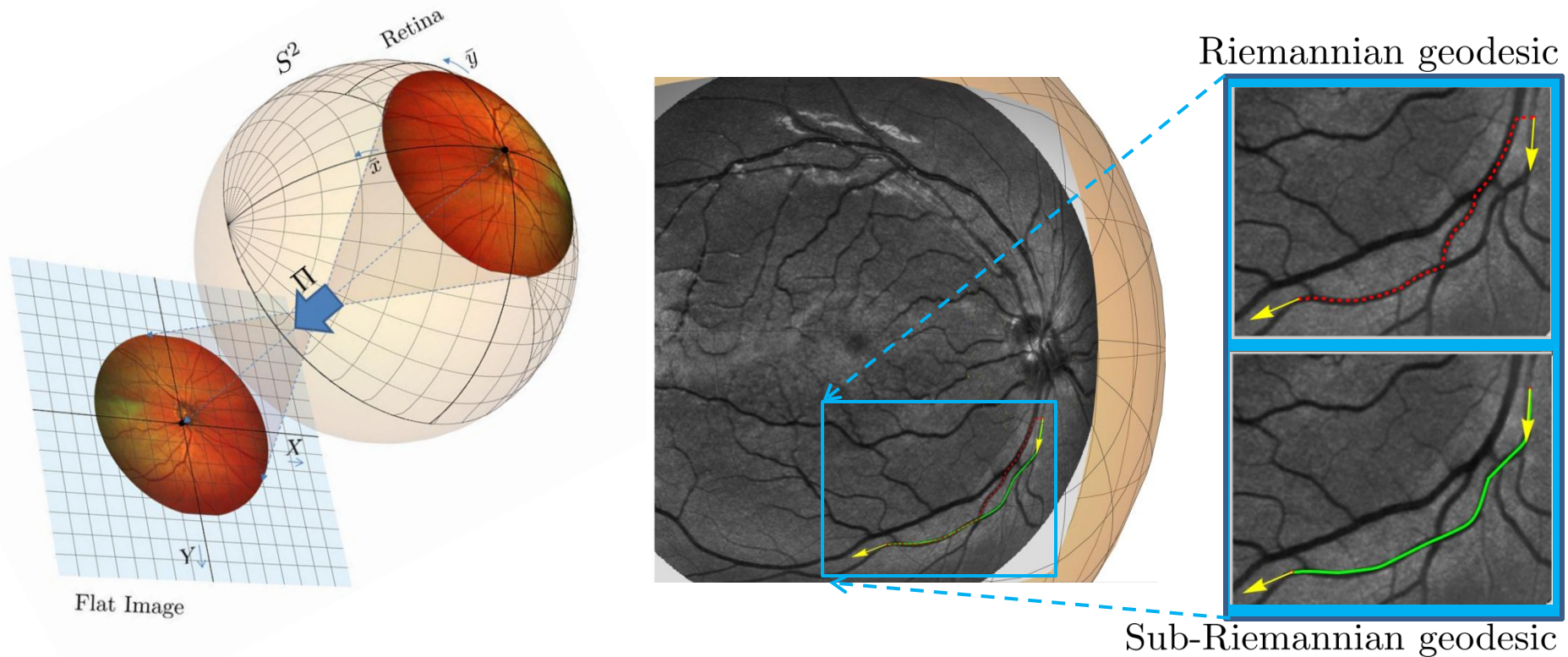
## Maxwell Set Exact



## Maxwell Set Numerically



# Tracking of Lines in Spherical Images via Sub-Riemannian Geodesics in $SO(3)$



[1] A. Mashtakov, R. Duits, Yu. Sachkov, E.J. Bekkers, I. Beschastnyi, *Tracking of Lines in Spherical Images via Sub-Riemannian Geodesics in  $SO(3)$* , JMIV, 2017.

[2] A.P. Mashtakov, R. Duits, Yu.L. Sachkov, E.J. Bekkers, I.Yu. Beschastnyi, *Sub-Riemannian Geodesics in  $SO(3)$  with Application to Vessel Tracking in Spherical Images of Retina*, Doklady Mathematics, 2017.



# Vessel Curvature via Data-driven SR-geodesics on SO(3)

$X_i$  - l.-i. v.f. on  $SO(3)$

$\mathcal{A}_i$  - l.-i. v.f. on  $SE(2)$

$\gamma^{SO(3)}$  -  $SO(3)$  geodesic

$\gamma^{SE(2)}$  -  $SE(2)$  geodesic

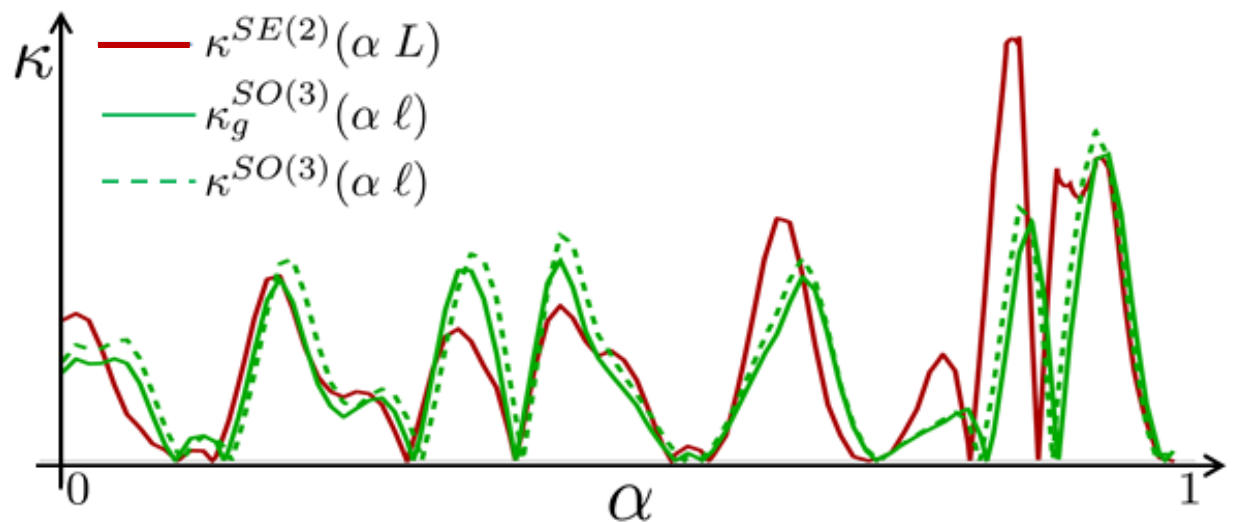
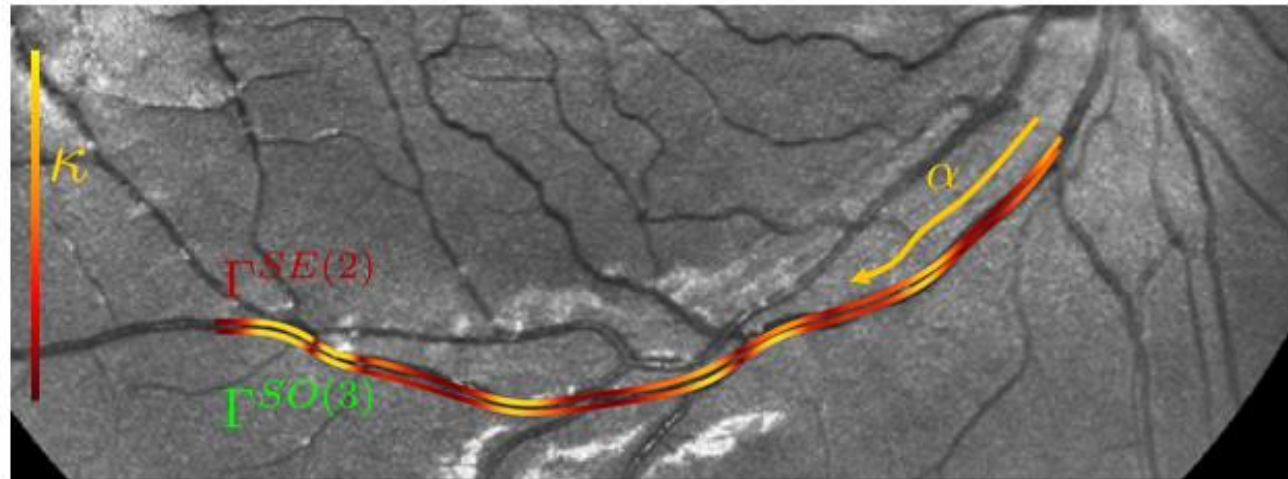
$\mathcal{W}$  - SR-distance  
from source point

Geodesic curvature

$$\begin{aligned}\kappa_g^{SO(3)}(\cdot) &= \\ &= -\xi^2 \frac{X_2|_{\gamma^{SO(3)}(\cdot)}(\mathcal{W}^{SO(3)})}{X_1|_{\gamma^{SO(3)}(\cdot)}(\mathcal{W}^{SO(3)})}\end{aligned}$$

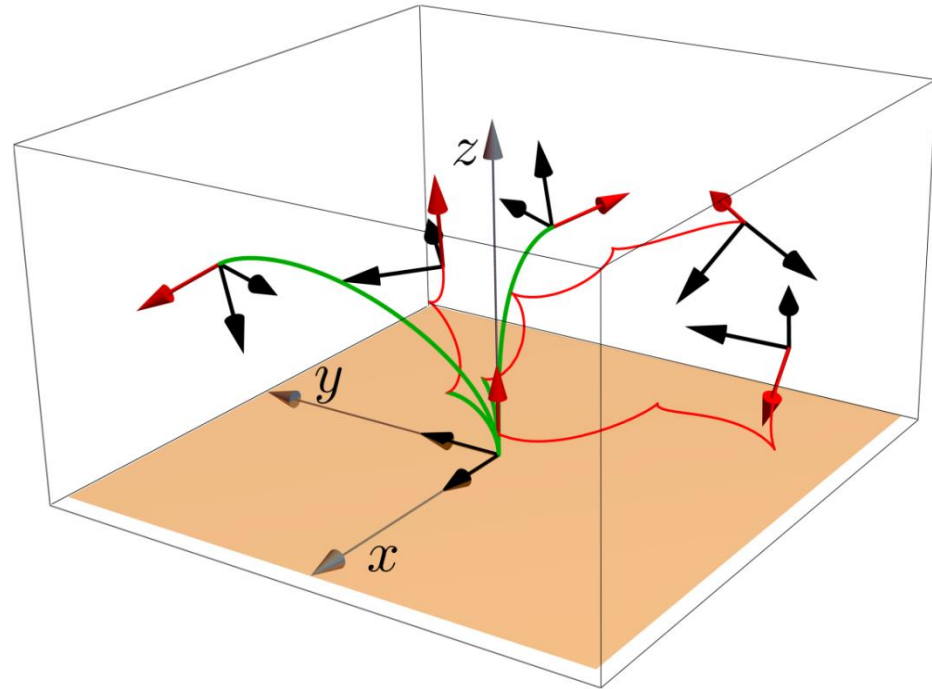
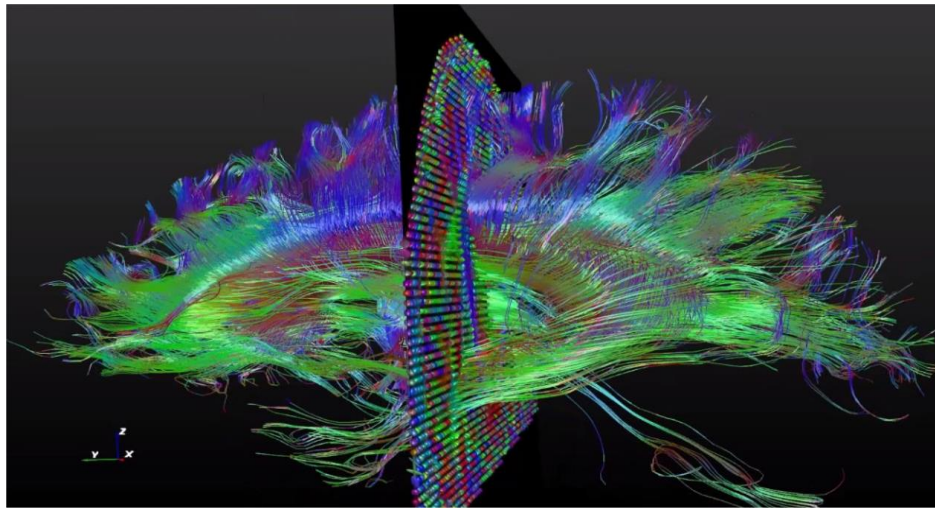
Plannar curvature

$$\begin{aligned}\kappa^{SE(2)}(\cdot) &= \\ &= -\xi^2 \frac{\mathcal{A}_2|_{\gamma^{SE(2)}(\cdot)}(\mathcal{W}^{SE(2)})}{\mathcal{A}_1|_{\gamma^{SE(2)}(\cdot)}(\mathcal{W}^{SE(2)})}\end{aligned}$$



# Sub-Riemannian geodesics on $SE(3)$

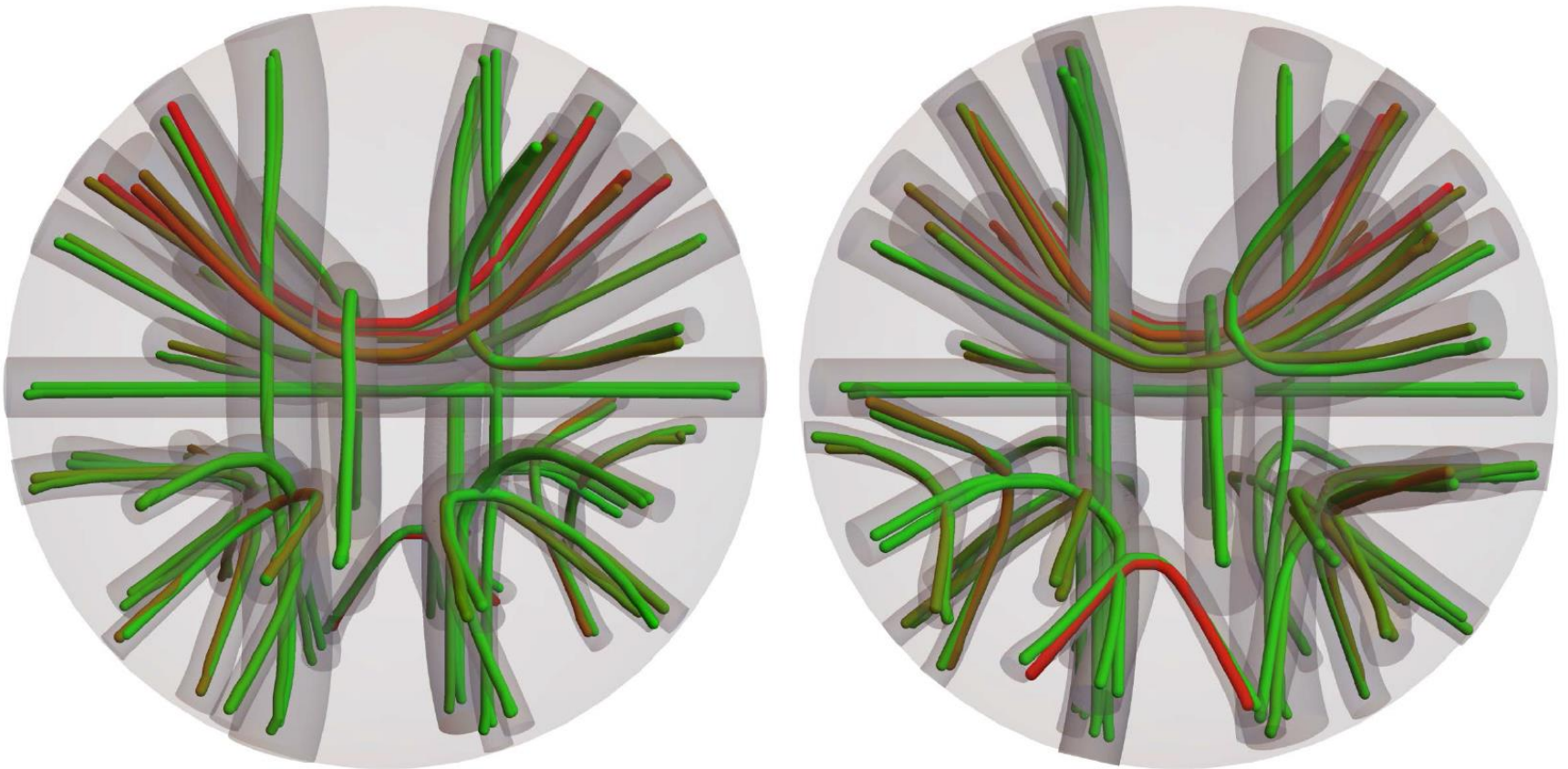
Data-driven sub-Riemannian geodesics on  $SE(3)$  are used for detection and analysis of neuron fibers in magnetic resonance images of a human brain.



[1] R. Duits, A. Ghosh, T. Dela Haije, A. Mashtakov,  
*On sub-Riemannian geodesics in  $SE(3)$  whose spatial projections do not have cusps*, JDCS, 2016.

[2] A. Mashtakov, A. Popov  
*Extremal Controls in the Sub-Riemannian Problem on the Group of Motions of Euclidean Space*, RCD, 2017.

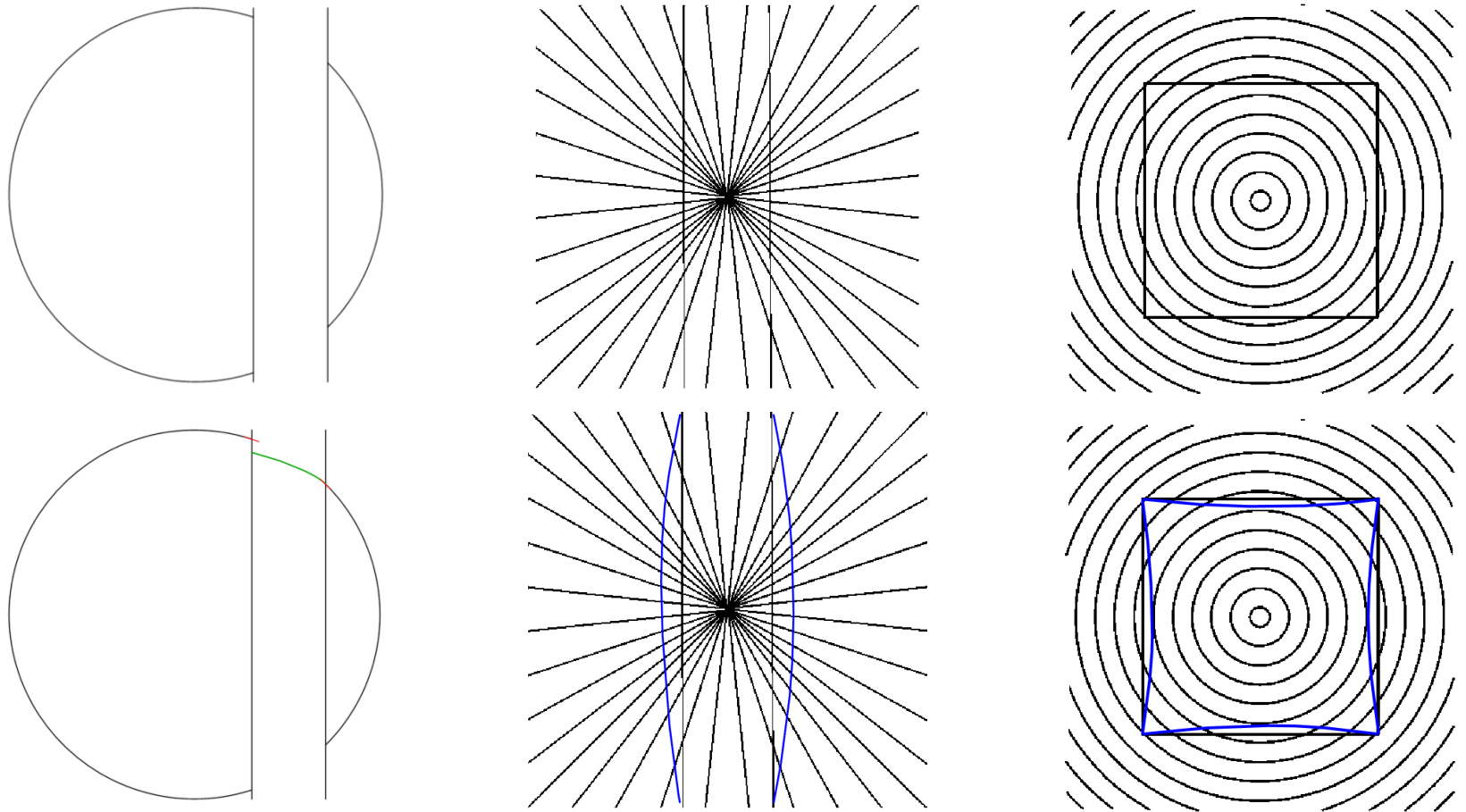
# Sub-Riemannian Fast Marching in SE(3)



Replicated from J. Portegies, S. Meesters, P. Ossenblok, A. Fuster, L. Florack, R. Duits.  
Brain Connectivity Measures via Direct Sub-Finslerian Front Propagation on the 5 D  
Sphere Bundle of Positions and Directions, MICCAI, 2018.

# Data-driven Sub-Riemannian Geodesics on $SE(2)$ for Modelling of Geometrical Optical Illusions

# GOIs via data-adaptive SR geodesics



- [1] B. Franceschiello, A. Mashtakov, G. Citti, A. Sarti, *Modelling of the Poggendorff Illusion via Sub-Riemannian Geodesics in the Roto-Translation Group*, LNCS, 2017.
- [2] B. Franceschiello, A. Mashtakov, G. Citti, A. Sarti, *Geometrical optical illusion via sub-Riemannian geodesics in the roto-translation Group*, DGA, 2019.



# Construction of External Cost

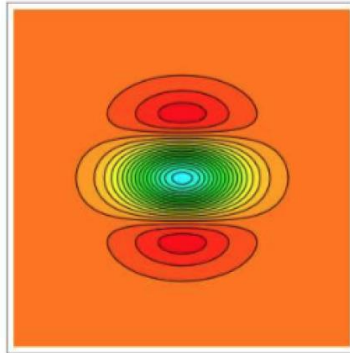
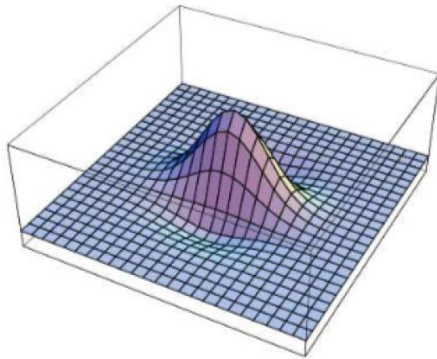
Retinal Plane  $\mathbb{R}^2 \ni (x, y)$ . Stimulus of Intensity  $I(x, y) : M \subset \mathbb{R}^2 \rightarrow \mathbb{R}^+$ .

Local coordinates  $\chi = (\chi_1, \chi_2) \in M$  centered at  $(x, y)$ .

Gabor Filters:

$$\psi_0(\chi) = \psi_0(\chi_1, \chi_2) = \frac{\alpha}{2\pi\sigma^2} e^{-\frac{(\chi_1^2 + \alpha^2 \chi_2^2)}{2\sigma^2}} e^{\frac{2i\chi_2}{\lambda}},$$

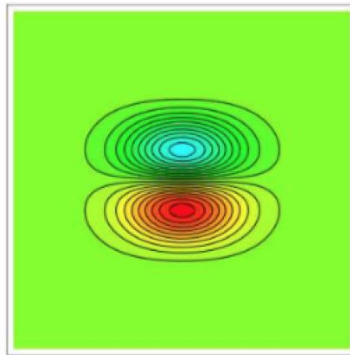
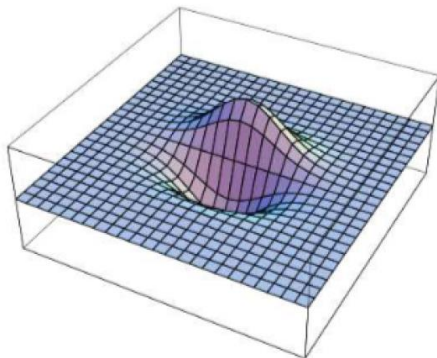
$\lambda > 0$  spatial wavelength,  $\alpha > 0$  spatial aspect ratio,  $\sigma > 0$  deviation.



Even part

$$\text{Re}(\psi_0(\chi)) = \frac{\alpha}{2\pi\sigma^2} e^{-\frac{(\chi_1^2 + \alpha^2 \chi_2^2)}{2\sigma^2}} \cos \frac{2\chi_2}{\lambda}$$

detection of contours.



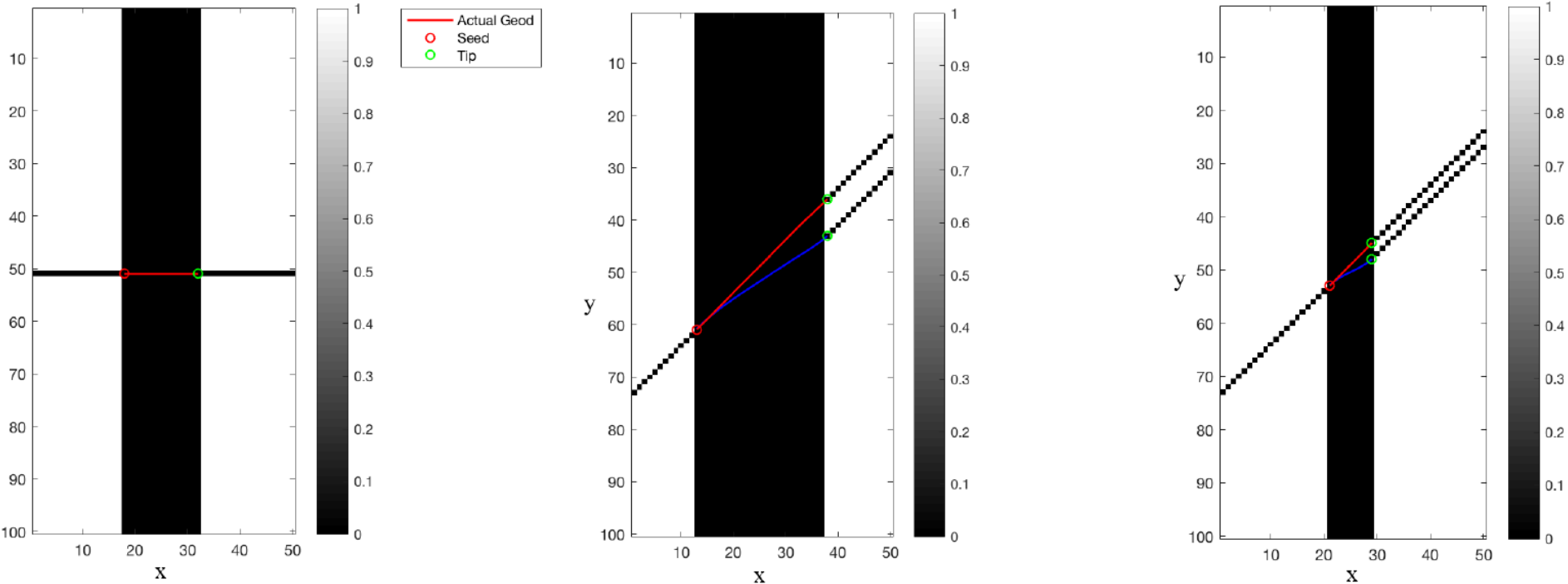
Odd part

$$\text{Im}(\psi_0(\chi)) = \frac{\alpha}{2\pi\sigma^2} e^{-\frac{(\chi_1^2 + \alpha^2 \chi_2^2)}{2\sigma^2}} \sin \frac{2\chi_2}{\lambda}$$

detection of boundaries.



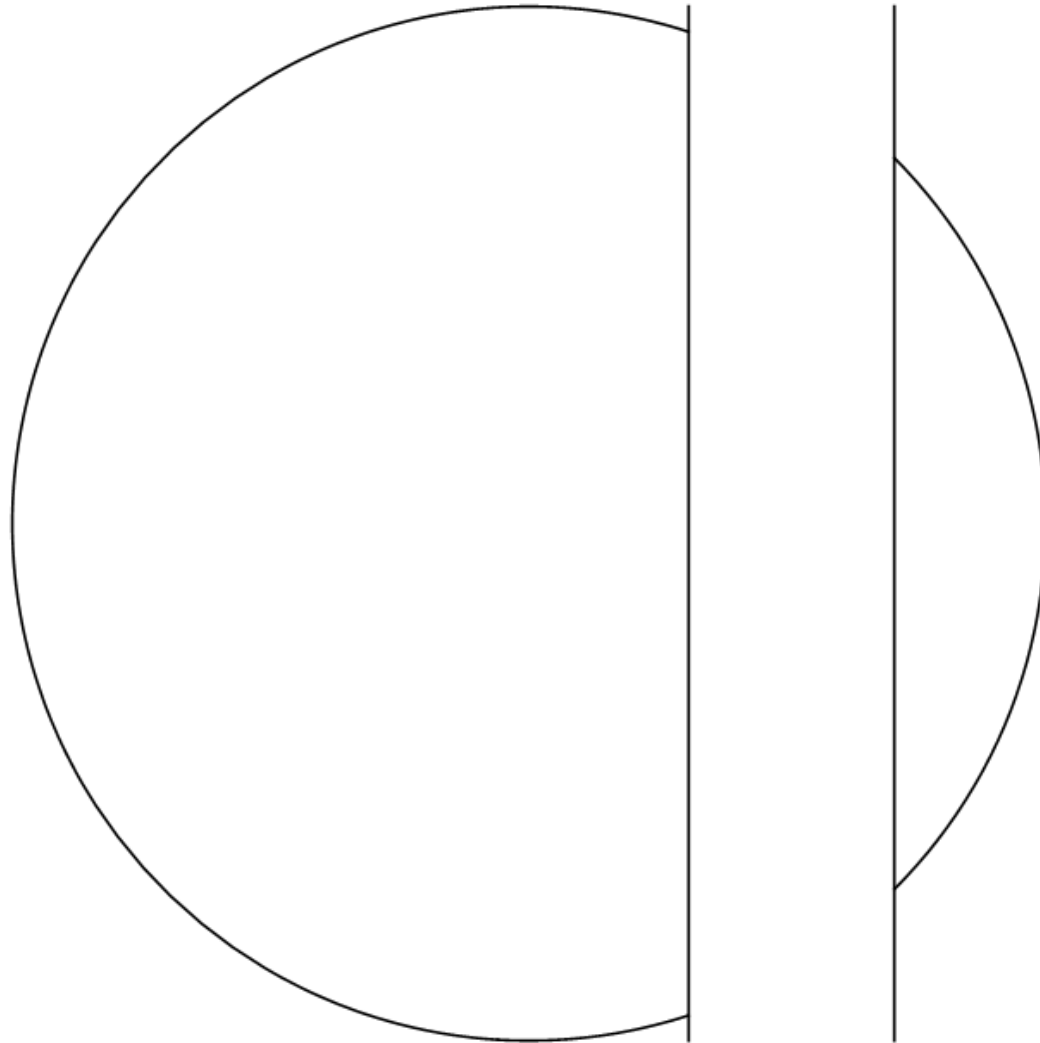
# Simulation of Illusory Contour



Type of curve	Width = 9 pixels	Width = 15 pixels	Width = 25 pixels
Percep. curve $\theta = \pi/4$	1.0366	1.8094	3.1113
Actual curve $\theta = \pi/4$	1.1369	2.0480	3.5354
Percep. curve $\theta = \pi/10$	2.1033	3.4719	4.9411
Actual curve $\theta = \pi/10$	2.8925	4.4927	7.3924
Percep. curve $\theta = \pi/2$	1.0320	1.4412	2.5196

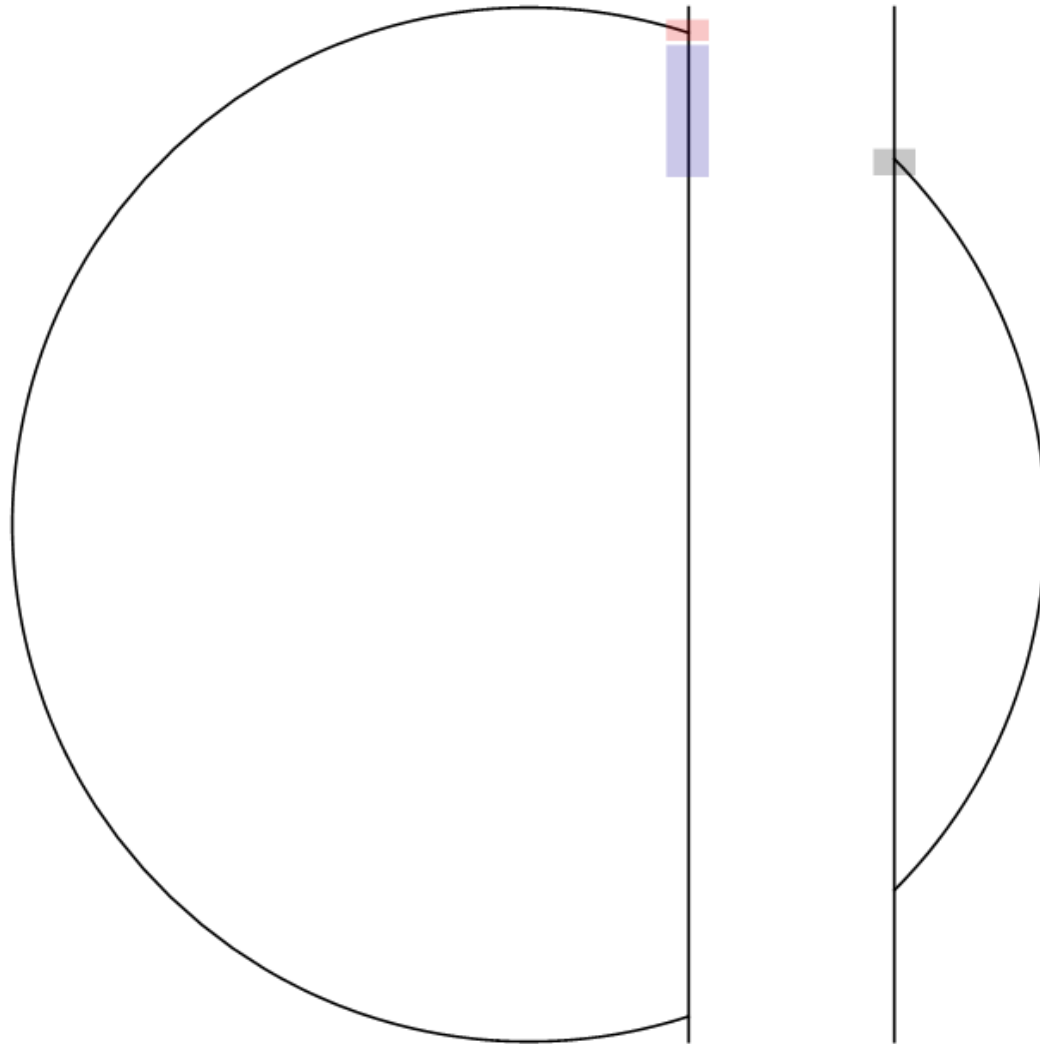
# Round Poggendorff Illusion

---



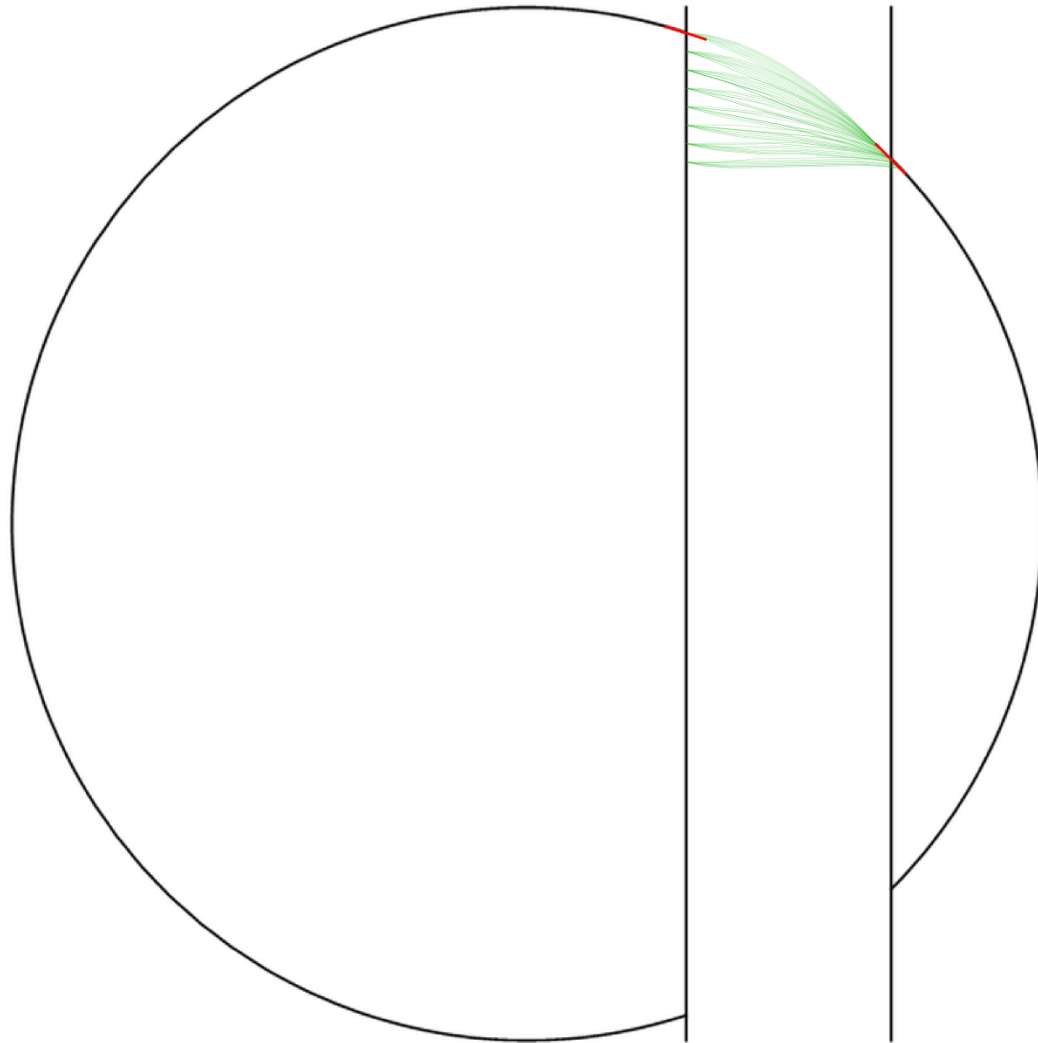
# Round Poggendorff Illusion

---



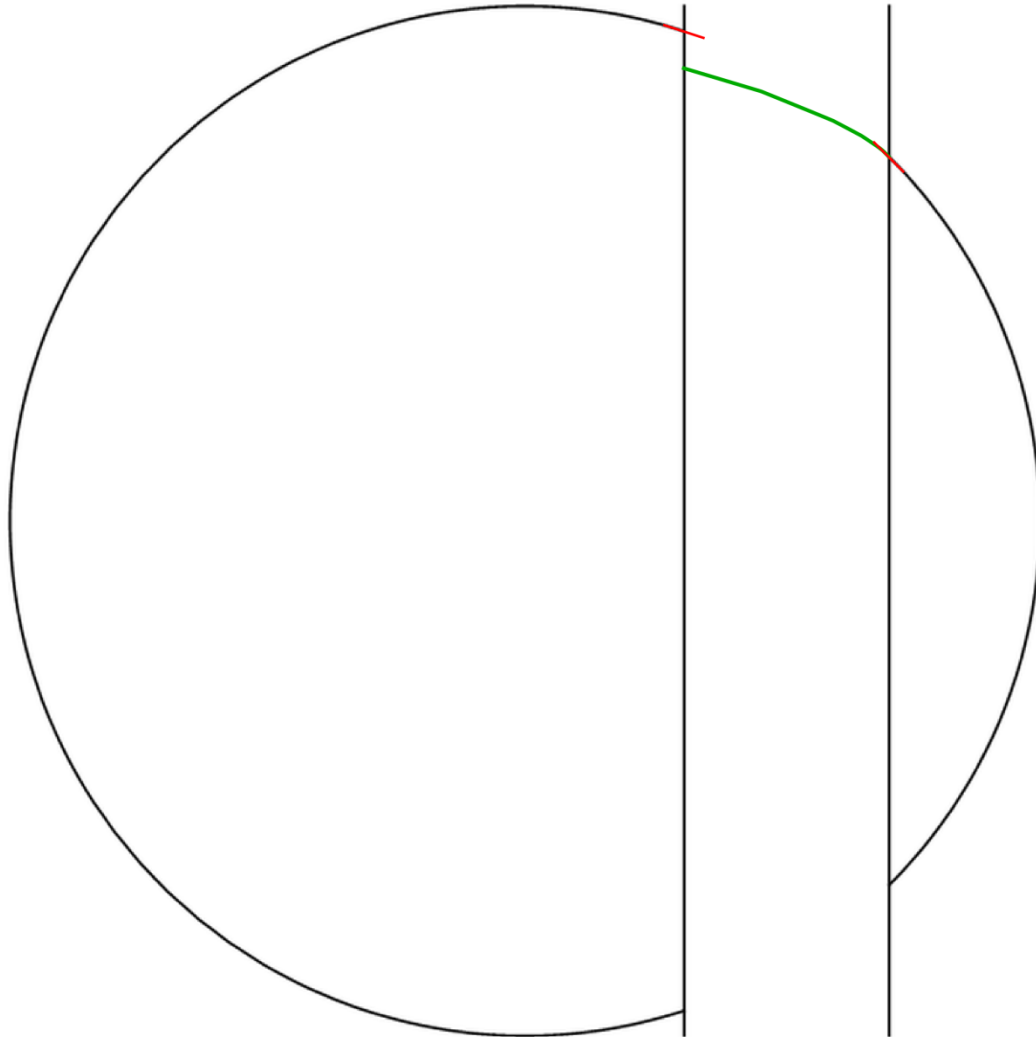
# Round Poggendorff Illusion

---



# Round Poggendorff Illusion

---



# Conclusion

- Sub-Riemannian geometry is a natural tool for brain inspired image processing.
- It is used for anthropomorphic image reconstruction.
- And for detection of salient lines and elongated structures in 2D and 3D images.
- Data-driven SR geodesics in  $SE(2)$  show promising results for vessel tracking in flat images of the retina.
- In  $SO(3)$  --- in spherical images of the retina.
- In  $SE(3)$  --- for fiber tracking in 3D MRI images of human brain.
- Including data-adaptivity refines the model of V1 and explains phenomena of GOI



**Thank you for your attention!**